A Study of Residual Stresses in Plane Strain Cold Rolling

by
Sharad Goyal

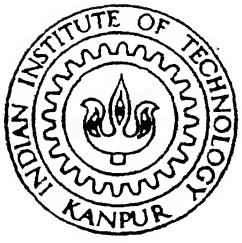

Department of Mechanical Engineering
Indian Institute of Technology Kanpur, India

January 1998

CERTIFICATE

It is certified that the work contained in the thesis entitled, ***A STUDY OF RESIDUAL STRESSES IN PLANE STRAIN COLD ROLLING***, by ***SHARAD GOYAL***, has been carried out under my supervision and that this work has not been submitted elsewhere for a degree.

Dr. P. M. Dixit
Professor
Department of Mechanical Engineering
I.I.T., Kanpur

Jan, 1998.

Acknowledgment

It is my pleasure, to acknowledge, indebeteness to Dr. P. M. Dixit, for his excellent guidance and active support, throughout the course of the thesis work.

Sincere thanks to friends, particularly Ajay, Suman Raaj, Surendra Gulati, U. S. Dixit, Vikas Gupta for their help in the times of need.

Thanks to everyone, for a memorable stay here.

Sharad Goyal

Contents

List of Figures

List of Tables

Nomenclature

A	Hardening parameter
$[B_L]$	Matrix relating the incremental linear strain to the incremental displacement
$[B_N]$	Matrix relating the incremental non-linear strain to the incremental displacement
$[C]$	Elastic stiffness matrix
$[C]^{EP}$	Elasto-plastic stiffness matrix
C_{ijkl}^{EP}	Elasto-plastic stiffness tensor
E	Young's modulus
$\{F\}$	Static force vector
K	hardening coefficient
$[K]$	Stiffness matrix
$[K_L]$	Linear part of the stiffness matrix
$[K_{NL}]$	Non-linear part of the stiffness matrix
N_i	Shape function of the element
$[Q]$	Matrix containing the shape functions of the element
S_{ij}	Piola-Kirchoff stress tensor
S_t	Surface of the body on which the stresses are specified
S_u	Surface of the body on which the displacements are specified
V	Volume of the body
$\{a\}$	Flow vector
$\{\mathrm{d}e\}$	Incremental Green-Lagrange strain vector
$\mathrm{d}e_{ij}$	Incremental Green-Lagrange strain tensor
$\mathrm{d}t$	Incremental time
$\mathrm{d}u$	Incremental displacement
$\{\mathrm{d}\epsilon\}$	Incremental natural strain vector
$\mathrm{d}\epsilon_{ij}$	Incremental natural strain tensor
$\{\mathrm{d}\sigma\}$	Incremental Cauchy stress vector
$\mathrm{d}\sigma_{ij}$	Incremental Cauchy stress tensor
$\{f\}$	Internal force vector

h_1	Initial thickness of strip
h_2	Final thickness of strip
n	Hardening exponent
r	% reduction
t	Time
$\tilde{u}$	Displacement vector
$\tilde{x}$	Position vector
$\Delta\eta_{ij}$	Incremental non-linear strain
ϵ^p_{eq}	Equivalent plastic strain
μ	Shear modulus
ν	Poisson's ratio
Ω_{ij}	Angular velocity tensor
ϕ_n	Neutral point angle
ρ	density
$\{\sigma'\}$	Deviatoric stress vector
σ_Y	Yield stress
σ_{eq}	Equivalent stress
σ_{ij}	Cauchy stress
σ'_{ij}	Deviatoric part of σ_{ij}
$\overset{\circ}{\sigma}_{ij}$	Jaumann stress rate

Abstract

To analyze the residual stresses in rolling, under plane strain condition, an updated Lagrangian elasto-plastic finite element formulation is presented. Inertial forces and roll deformation have not been considered. The material is assumed to yield according to the von-Mises criterion. Power-law type of strain hardening is used. Effect of temperature and strain rate on hardening behavior have been neglected. Friction at the roll-strip interface is incorporated only indirectly, as the boundary conditions at the interface are expressed in terms of incremental displacements. Parametric studies for change in reduction and the ratio of roll radius to strip thickness have been presented. The distribution of residual stresses is presented both over the domain (in the form of contours) as well as over the thickness.

Chapter 1

Introduction

Rolling can be considered as one of the most important processes in industry, and is at the same time one of the oldest metal-working processes. Strip rolling is a process in which thickness of a flat sheet is reduced by passing it between two counter-rotating cylinders which are separated by a fixed distance. The process may be performed at room temperature on a cold mill or at higher temperature on a hot mill, both of which may consist of one or more mill stands. In cold rolling, the roll radius is usually more than 50 times the initial strip thickness. If the width of the strip is at least five times the length of the arc of contact, the non-plastic material prevents the lateral spread, and the deformation takes place effectively under plane strain condition.

The complete analysis of rolling process is complex. As the strip enters the roll gap, first it deforms elastically. The relative velocity between the roll and the strip is such that frictional forces draw the metal in. The criterion of plastic flow governs the manner in which the transformation from elastic to plastic takes place. As the strip proceeds through the roll gap, more plastic flow occurs, until it comes out of the roll gap. The strip is then unloaded elastically. It is observed that the relative velocities of the roll and the strip change during the process. At the entry, the strip moves slower than the roll. As the strip starts accelerating forward, it reaches the surface velocity of the roll at the "no-slip" or neutral point, where the roll and strip move at the same speed. As the further compression occurs, the strip speeds up and the direction of friction changes in such a way that it now retards the motion. Tensions are often applied in cold rolling in order to ensure adequate control of the dimensional accuracy

of the rolled strip.

In rolling, the plastic deformation is often non-uniform. Therefore, to maintain the compatibility, different elements of the sheet cross-section unload to different levels of elastic deformation after they come out of the roll-gap. This induces self-equilibrating internal stresses in the sheet, called as residual stresses. It is generally believed that bad shape or poor flatness of rolled sheet is caused by residual stresses. Additionally, residual stresses have significant effects on further processing of the sheet. Thus, the distribution of residual stresses across the cross-section of cold rolled sheet plays an important role in rolling technology. The traditional method fail to predict residual stress distribution, because of the assumption of rigid-plastic material. The residual stresses can be taken into account by elasto-plastic finite-element analysis.

1.1 Literature Survey

To analyze the rolling process, numerous investigations, both analytical and experimental have been carried out. In view of the complexity of the process, analytical methods make use of several assumptions. These methods, therefore, provide useful but limited information.

Finite Element technique has been applied to analyze the rolling process in recent years. Most studies have used the Eulerian formulation, as it is found to be convenient for steady-state processes like rolling. Further, it takes much less computational time compared to the other formulation, namely updated Lagrangian formulation. Both the rigid-plastic as well as elasto-plastic constitutive equations have been used. A rigid plastic analysis in the Eulerian reference frame is found to be most suitable when the primary concern is to find the roll force, torque and inter-facial stresses. However, elastic effects must be taken into account when the objective is to find the plastic boundaries and residual stresses.

Eulerian elasto-plastic formulations have been reported by many authors. Dawson and Thompson (1978) have developed "initial stress rate" method. In this approach, the stress and velocity fields associated with the connective terms are assumed known and placed on the right-hand side of the finite element equations for momentum. An

iterative procedure is then used during which these terms are corrected until there is no discrepancy between the new stress distribution and the previous one. Variations are performed on pressure and velocity only. Results on residual stress distribution or plastic boundaries have not been reported.

Shimazaki and Thompson (1981) have used the mixed Eulerian formulation to solve for velocity, pressure and stress simultaneously. In their method, they have decoupled the momentum and continuity equations from the constitutive equation. The former set has been used to obtain velocity and pressure with stress assumed constant. The latter set has been used to obtain stress with velocity and pressure held constant. Iterations between these two sets are carried out until convergence. Thompson and Berman (1984) have employed the procedure developed by Shimazaki and Thompson (1981) for the analysis of plane-strain rolling. For a perfectly plastic material, analysis has been done for cold rolling. However, rate of convergence has been slow and results presented are without getting full convergence. Effective stress contours are plotted. but individual stress components have not been presented.

Abo-Elkhier et al. (1988) also have proposed an Eulerian formulation for solving elasto-plastic problem. For a linearly strain-hardening material, analysis for extrusion process has been conducted and some results on residual stresses are presented.

Thompson and Yu (1990) have presented an Eulerian formulation to solve the rate equilibrium equation, in their steady state form, for velocity and stress. The authors have used the formulation for the analysis of strip drawing for a perfectly plastic material. It is noted that the rate of convergence deteriorates as the inelastic response becomes large. Effective stress contours are plotted without getting full convergence. No result is presented for residual stress distribution.

Maniatty *et al.* (1991) have proposed an Eulerian elasto-plastic formulation in which the kinematics consists of a multiplicative decomposition of the deformation gradient into elastic and plastic components. Hart's (1976) constitutive model which contains an internal scalar variable, has been used for solving rolling and extrusion problems. In rolling problems a simple sliding friction law, $t_t = \beta(v_0 - v_t)$ where t_t is the traction on roll strip interface, v_o and v_t are the velocities of roll and strip respectively and β is friction coefficient is used. The system of equations is highly ill-conditioned and the algorithm lacks stability as the material becomes less rate sensitive.

An improved algorithm for solving the problem has been presented by Maniatty (1994) which makes use of discontinuous pressure field and allows the unknown nodal pressure to be eliminated from the formulation. Only longitudinal stress variation for a typical case is presented in these references [Maniatty *et al.*,1991,;Maniatty,1994]. Results for other components of residual stresses and hydrostatic pressure are not presented.

Malinowski and Lenard (1993) have proposed an elasto-plastic finite element scheme, using the Prandtl-Reuss constitutive relations, in an Eulerian-updated Lagrangian reference frame. Problem is solved in two stages, first the velocity field is determined by minimizing the total power of deformation and then the stresses are obtained by path line integration of the Jaumann stress rate. Path line integration, though an efficient method, gives unrealistic results due to non-satisfaction of equilibrium condition. A less efficient approach which involves minimization of a functional under certain constraints is used. Two types of shape functions (parabolic and Hermitian) are used and the results differ significantly from each other. In the proposed material model, Poisson's ratio is assumed to be a continuous material function defined both for elastic and elasto-plastic behavior. Malinowski (1993) has used the methodology developed by Malinowski and Lenard (1993) for determining residual stress distribution in plane strain cold rolling, in which roll deformation has also been taken into account. An additional functional is minimized iteratively for the roll deformation. Only limited results are presented and computational difficulties are not discussed.

Dixit and Dixit (1997) have reviewed various Eulerian elasto-plastic formulations and concluded that there are many unsolved difficulties in obtaining residual stresses using these formulations. They have proposed one simplified method to determine the more dominant longitudinal residual stress.

As far as the updated Lagrangian formulation is concerned, there are some studies on rolling [Liu *et al.*, 1985^a 1985^b] which use this formulation. But they have not studied the residual stress distribution.

1.2 Objective and Scope of the Present work

The present work is an attempt to study residual stress distribution in a cold rolling process. A large deformation elasto-plastic finite element (FE) technique is used. Even though the Eulerian formulation is convenient for such analysis and takes much less computational time than the updated Lagrangian formulation, here, the latter formulation is used. This is because, there are many un-solved difficulties with the convergence of the Eulerian formulation, especially in the unloading zone. Jaumann stress rate and Green-Lagrange strain tensors are used respectively as the measures of objective stress and non-linear strain. Newton-Raphson technique is used to solve the non-linear incremental equations of the updated Lagrangian formulation.

The material is assumed to yield according to von Mises criterion. Power-law type of strain-hardening relationship is used. The effects of strain rate and temperature on hardening behavior are ignored. Inertial forces, which have effect during the start up of the process, are not considered. Plane strain condition is assumed since the width to thickness ratio in strip rolling is usually more than five. Front and back tensions are not included in the analysis. For simplicity, rolls are considered to be rigid. Friction at the roll-strip interface is incorporated only indirectly, as boundary conditions on the interface are expressed in terms of incremental displacements.

A large deformation elasto-plastic updated Lagrangian FE code is first validated by comparing the results on roll torque and roll pressure distribution with the corresponding results of Eulerian rigid-plastic formulation. Residual stress distribution is obtained both over the domain (in the form of contours) as well as over the cross-section. Parametric study is carried out to study effects of reduction and the ratio of roll radius to strip thickness.

1.3 Plan of the thesis

Organization of the thesis is as follows:

In the second chapter, the updated Lagrangian formulation with material and geometric non-linearities and the corresponding finite element formulation, are presented.

The boundary conditions and evaluation of the secondary variables (roll pressure, roll torque, residual stresses, equivalent plastic strain) are discussed, at the end of the chapter.

In the third chapter, first the model is validated, then residual stress distribution is obtained and finally parametric study is carried out.

In the fourth chapter, conclusions of the present work as well as suggestions for the further work are presented.

Chapter 2

Finite Element Formulation for Large Deformation Elasto Plastic Analysis

In this chapter, the mathematical model of a large deformation elasto plastic problem is developed. The process is modeled as a steady state plane strain problem. The constitutive equation for the mechanical behavior of the work material is stated. The updated Lagrangian finite element formulation is developed.

2.1 Updated Lagrangian Formulation

In the study of deformation of a body subjected to external loading, often the original undeformed and unstressed configuration of the body is used for the formulation of its equation of motion. This is known as *Lagrangian Formulation.* This formulation is convenient for *small deformation* which is the case in a majority of engineering problems. In such cases, the deformed configuration does not deviate much from the original one and hence the deformation can be described by an infinitesimal strain tensor, known as the engineering strain tensor, for which the strain-displacement relation is *linear.*

On the other hand, for *large deformation* problems one has to use a finite strain measure which is expressed by a non-linear strain-displacement relation. Furthermore, the equations of motion,when expressed in the reference configuration, depend on the

deformation. Hence, for all large deformation problems, the Lagrangian Formulation proves to be cumbersome with the governing equations being difficult to solve. In such cases, one solves the problem using an incremental method known as *Updated Lagrangian Formulation*. In this formulation, it is assumed that the states of the stress and deformation of the body are known till the current configuration, say at time t. The main objective is then to determine the incremental deformation and stresses during an infinitesimal time step $\mathrm{d}t$, i. e. from time t to $t+\mathrm{d}t$. Here, the current configuration is used as the reference configuration for obtaining the incremental values. Unlike the Lagrangian Formulation, an incremental strain tensor is used. The methodology is particularly useful for elastic-plastic materials because the stress-strain relationship in such materials is usually expressed in an incremental fashion because of its dependence on the path of deformation.

2.2 Governing Equations

2.2.1 Strain-Displacement Relations

Figure (2.1) shows a strip element in its current configuration (which is being used as the reference configuration) at time t and a possible deformed configuration at time $t+\Delta t$. The vectors $\underline{u}^t$ and $\underline{u}^{t+\Delta t}$ denote the displacements of a point P of the body at time t and $t+\Delta t$. respectively. The position vectors of P at the above times are depicted as $\underline{x}^t$ and $\underline{x}^{t+\Delta t}$, respectively. For a very small value of Δt, one can represent it as $\mathrm{d}t$. Thus , from the figure it can be seen that $\underline{\mathrm{d}u}$ is the incremental displacement of P for the time step $\mathrm{d}t$. For small incremental deformation, one can represent the deformation tensorially using the following linear incremental strain tensor:

$$\mathrm{d}\epsilon_{ij} = \frac{1}{2}\left(\mathrm{d}u_{i,j} + \mathrm{d}u_{j,i}\right) \tag{2.1}$$

Note that $\mathrm{d}\epsilon_{ij}$ is not the incremental engineering strain tensor but the incremental logarithmic or natural strain tensor.

If the incremental deformation is large, the incremental strain-displacement relationship has to be non-linear, i. e. :

$$\mathrm{d}e_{ij} = \frac{1}{2}\left(\mathrm{d}u_{i,j} + \mathrm{d}u_{j,i} + \mathrm{d}u_{k,i}\mathrm{d}u_{k,j}\right) \tag{2.2}$$

The tensor de_{ij} is known as *Green Lagrange strain tensor.* Henceforth, the incremental displacement is assumed to be large and thus the non-linear strain-displacement relation given by eq. (2.2) is used.

2.2.2 Constitutive Equations

The plastic part of the incremental stress-strain relationship is obtained from the plastic potential of the material. For a material, yielding according to the von Mises criterion in an isotropic fashion, the plastic potential is given by Owen and Hinton (1980).

$$F(\sigma_{ij}, p) = \sigma_{eq}(\sigma_{ij}) - \sigma_y(p) \tag{2.3}$$

Note that

$$F = 0 \tag{2.4}$$

represents the yield criterion. The plastic potential F depends on the Cauchy stress tensor σ_{ij} through it's second invariant σ_{eq} called as equivalent stress and defined by

$$\sigma_{eq} = (\frac{3}{2}\sigma'_{ij}\sigma'_{ij})^{\frac{1}{2}} \tag{2.5}$$

where σ'_{ij} is the deviatoric part of σ_{ij}. Further, F depends on the variable yield stress of the material, σ_y , through a hardening variable p. For the case of strain hardening, p is identified as the equivalent plastic strain e^p_{eq}, and hence defined as :

$$p = e^p_{eq} = \int de^p_{eq} \tag{2.6}$$

and

$$de^p_{eq} = (\frac{2}{3}de^p_{ij}de^p_{ij})^{\frac{1}{2}} \tag{2.7}$$

Here, de^p_{ij} is the plastic part of the incremental strain tensor de_{ij} and the integration in eq.(2.6) is to be carried along the particle path. The dependence of σ_y on p (or e^p_{eq}) is normally approximated by a power-law type of relationship

$$\sigma_y - \sigma^0_y = K(e^p_{eq})^n \tag{2.8}$$

Here, K is called the hardening coefficient, n is called as the hardening exponent and σ_y^0 is the yield stress at zero plastic strain.

The incremental plastic strain (de_{ij}^p) is obtained from the plastic potential using the following relation :

$$de_{ij}^p = d\lambda \frac{\partial F}{\partial \sigma_{ij}} \tag{2.9}$$

where $d\lambda$ is a scalar. This equation is called as the flow rule. Differentiation of eq.(2.3) with respect to σ_{ij} gives

$$\frac{\partial F}{\partial \sigma_{ij}} = \frac{3}{2\sigma_{eq}} \sigma_{ij}^{'} \tag{2.10}$$

Using this and from eq.(2.9), one can determine $d\lambda$ as:

$$d\lambda = de_{eq}^p \tag{2.11}$$

Further, the hardening relationship and the yield condition (eq. 2.4) can be used to express $d\lambda$ as :

$$d\lambda = \frac{d\sigma_y}{H} = \frac{d\sigma_{eq}}{H} \tag{2.12}$$

where

$$H = \frac{d\sigma_y}{de_{eq}^p}, \tag{2.13}$$

the slope of the hardening curve, can be obtained from eq. (2.8). Substitution of eqs. (2.10) and (2.12) in eq. (2.9) leads to the following constitutive equation

$$de_{ij}^p = \frac{3}{2} \frac{d\sigma_{eq}}{H\sigma_{eq}} \sigma_{ij}^{'} \tag{2.14}$$

This constitutive relationship between the deviatoric stress tensor and the incremental plastic strain tensor is not really convenient for an updated Lagrangian formulation for which the incremental stress-strain relationship is needed. This can be obtained from eq. (2.14) as follows:

$$de_{ij}^p = \frac{3}{2} \frac{\sigma_{ij}^{'}}{H\sigma_{eq}} \frac{\partial \sigma_{eq}}{\partial \sigma_{kl}} d\sigma_{kl} \tag{2.15}$$

Note that,from eqs. (2.3) and (2.10), we get

$$\frac{\partial \sigma_{eq}}{\partial \sigma_{kl}} = \frac{\partial F}{\partial \sigma_{kl}} = \frac{3}{2\sigma_{eq}} \sigma_{kl}^{'}. \tag{2.16}$$

Substitution of eq. (2.16) in eq. (2.15) leads to the following incremental plastic stress-strain relationship :

$$de^p_{ij} = \frac{9\sigma'_{ij}\sigma'_{kl}}{4H\sigma^2_{eq}} d\sigma_{kl}. \tag{2.17}$$

The incremental elastic stress-strain relationship is given by

$$de^e_{ij} = \frac{1}{E}[-\nu d\sigma_{kk}\delta ij + (1+\nu)d\sigma_{ij}] \tag{2.18}$$

where de^e_{ij} is the elastic part of de_{ij} , E is the Young's modulus and ν is the Poisson's ratio. Adding the two relationships, we get

$$\begin{aligned} de_{ij} &= de^e_{ij} + de^p_{ij} \\ &= \left[-\frac{\nu}{E}\delta_{ij}\delta_{kl} + \frac{(1+\nu)}{E}\delta_{ik}\delta_{jl} + \frac{9\sigma'_{ij}\sigma'_{kl}}{4H\sigma^2_{eq}}\right] d\sigma_{kl} \end{aligned} \tag{2.19}$$

This is the incremental elastic-plastic stress-strain relationship needed in the updated Lagrangian formulation. However, it is the following inverse relationship [Chakrabarty (1987)] which is more useful :

$$d\sigma_{ij} = C^{EP}_{ijkl} de_{kl} \tag{2.20}$$

where

$$C^{EP}_{ijkl} = 2\mu\left[\delta_{ik}\delta_{jl} + \frac{\nu}{1-2\nu}\delta_{ij}\delta_{kl} - \frac{9\mu\sigma'_{ij}\sigma'_{kl}}{2(3\mu+H)\sigma^2_{eq}}\right] \tag{2.21}$$

and μ is the shear modulus related to E and ν by the relation:

$$\mu = \frac{E}{2(1+\nu)} \tag{2.22}$$

In eq (2.20), if the increment consists of only a pure rigid rotation, then $d\sigma_{ij}$ must be zero. A stress increment which satisfies this condition is called an *objective* stress increment. Thus, in the incremental elastic-plastic stress-strain relationship (eq. 2.20), the incremental stress tensor must be an objective stress tensor. The Cauchy stress tensor does not satisfy the objective requirement. So $d\sigma_{ij}$ in eq. (2.20) can not be interpreted as the incremental Cauchy stress-tensor. The two most commonly used objective stress tensors are (i) the *2nd Piola-Kirchoff* stress tensor S_{ij}, (ii) stress tensor whose material time derivative is given by the *Jaumann stress rate* $\overset{\circ}{\sigma}_{ij}$. If we use the latter, then $d\sigma_{ij}$ in eq. (2.20) should be identified as $\overset{\circ}{\sigma}_{ij}\, dt$. Thus

$$\overset{\circ}{\sigma}_{ij}\, dt = C^{EP}_{ijkl} de_{kl} \tag{2.23}$$

The Jaumann rate $\overset{\circ}{\sigma}_{ij}$ is related to Cauchy rate $\dot{\sigma}_{ij}$ by the relation

$$\overset{\circ}{\sigma}_{ij}\, \mathrm{d}t = \dot{\sigma}_{ij}\mathrm{d}t - \sigma_{ik}(\Omega_{jk}\mathrm{d}t) - \sigma_{jk}(\Omega_{ik}\mathrm{d}t) \tag{2.24}$$

where the incremental rotation tensor $(\Omega_{ij}\mathrm{d}t)$ is defined as

$$\Omega_{ij}\mathrm{d}t = \frac{1}{2}(\mathrm{d}u_{i,j} - \mathrm{d}u_{j,i}). \tag{2.25}$$

Equations (2.21, 2.23-2.25) represent the elastic-plastic incremental stress-strain relationship to be used in the updated Lagrangian formulation.

2.2.3 Equilibrium Equations

In a steady state problem. inertial forces are negligible. Neglecting body forces also, the equilibrium equation becomes

$$\sigma_{ij,j} = 0. \tag{2.26}$$

This equation is to be satisfied in the deformed configuration (i. e. in the configuration at time t+dt) which is not known yet. In updated Lagrangian formulation, we need equilibrium equation in terms of the incremental stress. The incremental form of eq. (2.26) is given by Hill (1950).

$$\mathrm{d}\sigma_{ij,j} - (\sigma_{ij,k})\mathrm{d}u_{k,j} = 0. \tag{2.27}$$

Note that $\mathrm{d}\sigma_{ij}$ in the above equation is the incremental Cauchy stress tensor and hence equal to $\overset{\circ}{\sigma}_{ij}\, \mathrm{d}t$.

2.2.4 Incremental Governing Equations

It is assumed that the strip passes through the roll gap in several increments, and after a certain number of increments, we arrive at the current configuration (i. e. the configuration at the present time t), which is treated as the reference configuration (see fig. 2.1). Further, the displacement vector u_i and the stress tensor σ_{ij} at the present time are known. Now a incremental displacement is applied to the boundary of the current configuration. Then to find the resulting incremental displacements, strains and stresses $(\mathrm{d}u_i, \mathrm{d}\epsilon_{ij}, \mathrm{d}\sigma_{ij})$, we have to solve the following equations:

(a) Incremental equilibrium equations:

$$d\sigma_{ij,j} - (\sigma_{ij,k})du_{k,j} = 0; \tag{2.28}$$

(b) Incremental stress-strain relations:

$$\overset{\circ}{\sigma}_{ij}\, dt = C^{EP}_{ijkl} de_{kl}; \tag{2.29}$$

[$\overset{\circ}{\sigma}_{ij}$ defined by eqs. (2.24-2.25) and C^{EP}_{ijkl} defined by eq. (2.21)]

(c) Incremental strain-displacement relations:

$$de_{ij} = \frac{1}{2}(du_{i,j} + du_{j,i} + du_{k,i}du_{k,j}) \tag{2.30}$$

2.3 Finite Element Formulation

In this section, a finite element formulation corresponding to the incremental equations of the updated Lagrangian approach of section 2.2 has been developed. First, an elastic-plastic matrix relating incremental stress and strain vectors is derived using the plastic potential proposed in section 2.2.2. Then, the equilibrium equations in the deformed configuration are derived using the principle of virtual work following a procedure given in Bathe et al (1975). Finally, the numerical scheme required to solve the finite element equations is discussed.

2.3.1 Incremental Stress-Strain Relationship Representing Material Non-linearity

The incremental stress-strain relation can be expressed in vector form as

$$\{d\sigma\} = [C]^{EP}\{de\} \tag{2.31}$$

where

$$\{d\sigma\}^T = \{d\sigma_{xx}, d\sigma_{yy}, d\sigma_{xy}, d\sigma_{zz}\} \tag{2.32}$$

and

$$\{de\}^T = \{de_{xx}, de_{yy}, 2de_{xy}, de_{zz}\} \tag{2.33}$$

are respectively the vector forms of the incremental (objective) stress and strain tensors. The expression for the elastic-plastic matrix $[C^{EP}]$ is derived from the plastic potential F. For its derivation, it is convenient to express the yield condition eqs. (2.3) and (2.4) as

$$F(\{\sigma\},p) \equiv \sigma_{eq}(\{\sigma\}) - \sigma_y(p) = 0 \tag{2.34}$$

where

$$\{\sigma\}^T = \{\sigma_{xx}, \sigma_{yy}, \sigma_{xy}, \sigma_{zz}\} \tag{2.35}$$

On the yield surface, $\mathrm{d}F = 0$ and hence

$$(\frac{\partial F}{\partial\{\sigma\}})^T\{\mathrm{d}\sigma\} + \frac{\partial F}{\partial p}\mathrm{d}p = 0 \tag{2.36}$$

or

$$\{a\}^T\{\mathrm{d}\sigma\} - A\mathrm{d}\lambda = 0 \tag{2.37}$$

where, the flow vector $\{a\}$ is defined by

$$\{a\} = \frac{\partial F}{\partial\{\sigma\}}, \tag{2.38}$$

the parameter A is given by

$$A = -\frac{1}{\mathrm{d}\lambda}\frac{\partial F}{\partial p}\mathrm{d}p, \tag{2.39}$$

and $\mathrm{d}\lambda$ is the same scalar which appears in eq. (2.9). Eq. (2.10) gives the following expression for the flow vector:

$$\{a\} = \frac{3}{2\sigma_{eq}}\{\sigma\}'. \tag{2.40}$$

where $\{\sigma\}'$ is the vector form of the deviatoric part of σ_{ij}. Eqs. (2.6) and (2.11) give

$$\mathrm{d}p = \mathrm{d}\lambda = \mathrm{d}e^p_{eq}. \tag{2.41}$$

Substitution of eqs. (2.34) and (2.41) in eq. (2.39) leads to the following expression for A:

$$A = \frac{\mathrm{d}\sigma_y}{\mathrm{d}p} = \frac{\mathrm{d}\sigma_y}{\mathrm{d}e^p_{eq}} \tag{2.42}$$

The total strain increment can be split into elastic and plastic parts. Thus

$$\{\mathrm{d}e\} = \{\mathrm{d}e^e\} + \{\mathrm{d}e^p\} = [C]^{-1}\{\mathrm{d}\sigma\} + \mathrm{d}\lambda\frac{\partial F}{\partial\{\sigma\}}$$

$$= [C]^{-1}\{d\sigma\} + d\lambda\{a\} \tag{2.43}$$

Here, $[C]$ is the matrix form of the elasticity tensor C_{ijkl} (See eq. 2.18). The second part of the right hand of eq. (2.43) is due to the flow rule (eq. 2.9). Premultiplying both sides of equation (2.43) by $\{a\}^T[C]$ and using eq. (2.37), we get

$$d\lambda = \frac{\{a\}^T[C]\{de\}}{A + \{a\}^T[C]\{a\}} \tag{2.44}$$

Substituting the above expression for $d\lambda$ in eq. (2.43), we get

$$\{de\} = [C]^{-1}\{d\sigma\} + \frac{\{a\}^T[C]\{de\}}{A + \{a\}^T[C]\{a\}}\{a\} \tag{2.45}$$

which leads to

$$\{d\sigma\} = \left([C] - \frac{[C]\{a\}\{a\}^T[C]}{A + \{a\}^T[C]\{a\}}\right)\{de\} \tag{2.46}$$

Therefore,

$$[C]^{EP} = \left([C] - \frac{[C]\{a\}\{a\}^T[C]}{A + \{a\}^T[C]\{a\}}\right) \tag{2.47}$$

where the expression for $\{a\}$ is given by eq. (2.40). For a material with power strain hardening law (eq. 2.8), the expression (2.42) for A reduces to

$$A = K\,n(e^p_{eq})^{n-1} \tag{2.48}$$

For an isotropic material, the expression for $[C]$ for plane strain case is given by

$$[C] = \frac{E}{(1+\nu)(1-2\nu)}\begin{bmatrix} 1-\nu & \nu & 0 & \nu \\ \nu & 1-\nu & 0 & \nu \\ 0 & 0 & \frac{1-2\nu}{2} & 0 \\ \nu & \nu & 0 & 1-\nu \end{bmatrix} \tag{2.49}$$

As stated at the end of subsection 2.2.2, the vector $\{d\sigma\}$ in eq. (2.46) should be interpreted as an objective stress increment.

2.3.2 Updated Lagrangian Formulation for Geometric Non-Linearity

When a body experiences a large deformation and/or rotation, the equilibrium must be established in the current configuration. As stated earlier, the normal solution

procedure adopted in this case is updated Lagrangian. That is to say that when all the kinematical variables are known from time 0 to time t in discrete time steps, the objective is to establish the equilibrium in the configuration at time $t+\Delta t$. In order to derive the finite element equilibrium equations at time $t+\Delta t$, the principle of virtual work requires that

$$\int_{V^{t+\Delta t}} \sigma_{ij}^{t+\Delta t}\, \delta(\epsilon_{ij}^{t+\Delta t})\, \mathrm{d}V^{t+\Delta t} = R^{t+\Delta t} \tag{2.50}$$

where $\sigma_{ij}^{t+\Delta t}$ is the Cauchy stress tensor at time $t+\Delta t$, $\delta(\epsilon_{ij}^{t+\Delta t})$ is the virtual infinitesimal strain tensor at time $t+\Delta t$, $R^{t+\Delta t}$ is the virtual work of the surface forces at time $t+\Delta t$ (body forces being neglected) and $V^{t+\Delta t}$ is the domain at time $t+\Delta t$. The major difficulty in application of eq. (2.50) is that the configuration at $t+\Delta t$ is unknown. Moreover quantities like Cauchy stress tensor are not purely additive as one has to take care of rotation into account.

An elegant way of formulating the problem is given by Bathe et al (1975). Here, the virtual work expression (eq. 2.50) is transformed to an integral over the known domain at time t (i. e. V_t) using the 2nd Piola- Kirchoff stress tensor and the Green-Lagrange strain tensor. Thus, the virtual work expression becomes

$$\int_{V_t} {}_tS_{ij}^{t+\Delta t}\, \delta({}_te_{ij}^{t+\Delta t})\, \mathrm{d}V^t = R^{t+\Delta t}. \tag{2.51}$$

where S_{ij} denotes the 2nd Piola- Kirchoff stress tensor whose relation with the Cauchy stress tensor σ_{ij} is given by

$${}_tS_{ij}^{t+\Delta t} = \frac{\rho^t}{\rho^{t+\Delta t}}({}_{t+\Delta t}r_{i,m}^t)\, \sigma_{mn}^{t+\Delta t}({}_{t+\Delta t}r_{j,n}^t). \tag{2.52}$$

[The right superscript stands for the current configuration and the left subscript denotes the reference configuration.]

Since the Cauchy stress tensor is always referred to the current configuration, the left subscript has been omitted. Here ${}_{t+\Delta t}x_{i,m}^t$ represents the derivative of the position vector $\underline{x}^t$ at time t with respect to the one ($\underline{x}^{t+\Delta t}$) at time $t+\Delta t$ and $\frac{\rho^t}{\rho^{t+\Delta t}}$ denotes the ratio of densities at time t and $t+\Delta t$. The Green-Lagrange strain tensor ${}_te_{ij}^{t+\Delta t}$ is defined as

$${}_te_{ij}^{t+\Delta t} = \frac{1}{2}\left({}_tu_{i,j}^{t+\Delta t} + {}_tu_{j,i}^{t+\Delta t} + {}_tu_{k,i}^{t+\Delta t}\,{}_tu_{k,j}^{t+\Delta t}\right) \tag{2.53}$$

where ${}_tu_{i,j}^{t+\Delta t}$ is the derivative of the displacement vector $\underline{u}^{t+\Delta t}$ at time $t+\Delta t$ with respect to the position vector at time t.

An incremental decomposition of stress and strain gives

$$
\begin{aligned}
{}_tS_{ij}^{t+\Delta t} &= {}_tS_{ij}^{t} + {}_t\Delta S_{ij} \\
&= \sigma_{ij}^{t} + {}_t\Delta S_{ij}, \qquad (2.54)
\end{aligned}
$$

$$
\delta_t e_{ij}^{t+\Delta t} = \delta_t \Delta\epsilon_{ij} + \delta_t \Delta\eta_{ij}, \qquad (2.55)
$$

where,

$$
{}_t\Delta\epsilon_{ij} = \frac{1}{2}\left({}_t\Delta u_{i,j} + {}_t\Delta u_{j,i}\right) \qquad (2.56)
$$

and

$$
{}_t\Delta\eta_{ij} = \frac{1}{2}\left({}_t\Delta u_{k,i}\right)\left({}_t\Delta u_{k,j}\right). \qquad (2.57)
$$

Here ${}_t\Delta u_{i,j}$ stands for the derivative of ${}_t\Delta\underline{u}$ (incremental displacement vector at time t) with respect to $\underline{x}^t$ (position vector at time t). Thus, eq. (2.51) with incremental decomposition can be written as

$$
\begin{aligned}
\int_{V^t} {}_t\Delta S_{ij}\delta({}_t\Delta\epsilon_{ij})\mathrm{d}V^t + \int_{V^t} {}_t\Delta S_{ij}\delta({}_t\Delta\eta_{ij})\mathrm{d}V^t + \int_{V^t} \sigma_{ij}^t\delta({}_t\Delta\eta_{ij})\mathrm{d}V^t \\
+ \int_{V^t} \sigma_{ij}^t\delta({}_t\Delta\epsilon_{ij})\mathrm{d}V^t = R^{t+\Delta t}. \qquad (2.58)
\end{aligned}
$$

The 2nd integral on the left hand side is a higher order term compared to other terms and hence can be neglected. Moreover, using an elastic-plastic incremental stress-strain relationship (eq. 2.20), ${}_t\Delta S_{ij}$ can be approximated as ${}_tC_{ijkl}^{EP}\,{}_t\Delta\epsilon_{kl}$. Here, the left subscript of ${}_tC_{ijkl}^{EP}$ denotes the time at which it is to be evaluated. The above simplification will definitely give rise to an error in the right hand side of eq. (2.58). The error is normally neutralized by using some iterative scheme like Newton Raphson Method. Now, eq. (2.58) can be written as

$$
\begin{aligned}
\int_{V^t} {}_tC_{ijkl}^{EP}{}_t\Delta\epsilon_{kl}\delta({}_t\Delta\epsilon_{ij})\mathrm{d}V^t + \int_{V^t} \sigma_{ij}^t\delta({}_t\Delta\eta_{ij})\mathrm{d}V^t + \int_{V^t} \sigma_{ij}^t\delta({}_t\Delta\epsilon_{ij})\mathrm{d}V^t \\
= R^{t+\Delta t}. \qquad (2.59)
\end{aligned}
$$

Owing to the symmetries in ${}_tC_{ijkl}^{EP}$, ${}_t\Delta\epsilon_{ij}$, ${}_t\Delta\eta_{ij}$ and σ_{ij}^t, eq. (2.59) can be rewritten in the following form:

$$
\begin{aligned}
\int_{V^t} \left(\delta_t\{\Delta\epsilon\}^T\right){}_t[C]^{EP}{}_t\{\Delta\epsilon\}\mathrm{d}V^t + \int_{V^t} \left(\delta_t\{\Delta\eta\}^T\right)[T]^t{}_t\{\Delta\eta\}\mathrm{d}V^t \\
+ \int_{V^t} \left(\delta_t\{\Delta\epsilon\}^T\right)\{\sigma\}^t\mathrm{d}V^t = R^{t+\Delta t}. \qquad (2.60)
\end{aligned}
$$

where,

$$ {}_t\{\Delta\epsilon\} = \{{}_t\Delta\epsilon_{xx},\ {}_t\Delta\epsilon_{yy},\ 2_t\Delta\epsilon_{xy},\ {}_t\Delta\epsilon_{zz}\}^T, \tag{2.61} $$

$$ \{\sigma\}^t = \{\sigma^t_{xx},\ \sigma^t_{yy},\ \sigma^t_{xy},\ \sigma^t_{zz}\}^T, \tag{2.62} $$

$$ {}_t\{\Delta\eta\} = \{{}_t\Delta u_{x,x},\ {}_t\Delta u_{x,y},\ {}_t\Delta u_{x,z},\ {}_t\Delta u_{y,x},\ {}_t\Delta u_{y,y},\ {}_t\Delta u_{y,z},\}^T, \tag{2.63} $$

$$ [T]^t = \begin{bmatrix} [\Sigma]^t & 0 \\ 0 & [\Sigma]^t \end{bmatrix} \tag{2.64} $$

and

$$ [\Sigma]^t = \begin{bmatrix} \sigma^t_{xx} & \sigma^t_{xy} & 0 \\ \sigma^t_{yx} & \sigma^t_{yy} & 0 \\ 0 & 0 & \sigma^t_{zz} \end{bmatrix} \tag{2.65} $$

The ${}_t[C]^{EP}$ matrix is the elastic-plastic matrix evaluated at time t which is given by eq. (2.47).

2.3.3 Finite Element Equations

The domain is discretized into a number of elements and the incremental displacement field over a typical element e is approximated as

$$ {}_t\{\Delta u\} = [Q]\,{}_t\{\Delta u\}^e \tag{2.66} $$

where,

$$ {}_t\{\Delta u\}^e = \{{}_t\Delta u^1_x,\ {}_t\Delta u^1_y, \ldots, {}_t\Delta u^n_x,\ {}_t\Delta u^n_y\}. $$

and ${}_t\Delta u^i_x$, ${}_t\Delta u^i_y$ stand for the (unknown) incremental displacements of node 'i' in x and y directions respectively . Here

$$ [Q] = \begin{bmatrix} \{Q_1\}^T \\ \{Q_2\}^T \end{bmatrix} \tag{2.67} $$

where

$$ \begin{aligned} \{Q_1\}^T &= \begin{bmatrix} N_1 & 0 & N_2 & 0 & \ldots & N_n & 0 \end{bmatrix}, \\ \{Q_2\}^T &= \begin{bmatrix} 0 & N_1 & 0 & N_2 & \ldots & 0 & N_n \end{bmatrix}. \end{aligned} \tag{2.68} $$

and N_i, the functions of (x, y), are called the *shape functions.*

With displacement field defined by eq. (2.66), the strain field within the element can be calculated in terms of nodal displacements. From eq. (2.66),

$$ {}_t\Delta u_{i,j} = \frac{\partial_t \Delta u_i}{\partial^t x_j} = {}_t\{Q_i\}^T_{,j}\, {}_t\{\Delta u\}^e \tag{2.69} $$

where

$$ {}_t\{Q_i\}^T_{,j} = \frac{\partial \{Q_i\}^T}{\partial^t x_j}. \tag{2.70} $$

Substituting eq. (2.69) in eqs. (2.56) and (2.57) and arranging them in vector form, we get the strain displacement relations:

$$ {}_t\{\Delta\epsilon\} = {}_t[B_L]\, {}_t\{\Delta u\}^e, \tag{2.71} $$

$$ {}_t\{\Delta\eta\} = {}_t[B_N]\, {}_t\{\Delta u\}^e \tag{2.72} $$

where,

$$ {}_t[B_L] = \begin{bmatrix} {}_t\{Q_1\}^T_{,x} \\ {}_t\{Q_2\}^T_{,y} \\ {}_t\{Q_2\}^T_{,x} + {}_t\{Q_1\}^T_{,y} \\ 0 \end{bmatrix} \tag{2.73} $$

and

$$ {}_t[B_N]^T = \begin{bmatrix} {}_t\{Q_1\}_{,x} & {}_t\{Q_1\}_{,y} & 0 & {}_t\{Q_2\}_{,x} & {}_t\{Q_2\}_{,y} & 0 \end{bmatrix} \tag{2.74} $$

Using the strain displacement relations derived above, the contribution to the integral (eq. 2.60) from a typical element e (with volume V_e^t) can be written as

$$ \begin{aligned} \delta_t\{\Delta u\}^{eT} \left(\int_{V_e^t} {}_t[B_L]^T\, {}_t[C]^{EP}\, {}_t[B_L]\, \mathrm{d}V^t \right) {}_t\{\Delta u\}^e + \\ \delta_t\{\Delta u\}^{eT} \left(\int_{V_e^t} {}_t[B_N]^T\, [T]^t\, {}_t[B_N]\, \mathrm{d}V^t \right) {}_t\{\Delta u\}^e + \\ \delta_t\{\Delta u\}^{eT} \left(\int_{V_e^t} {}_t[B_L]^T\, \{\sigma\}^t\, \mathrm{d}V^t \right) = \delta_t\{\Delta u\}^{eT}\ ({}_{t+\Delta t}\{F\}^e) \end{aligned} \tag{2.75} $$

Here, the contribution to the term $R^{t+\Delta t}$ from the element e has been expressed in terms of the elemental external force vector ${}_{t+\Delta t}\{F\}^e$ using a standard procedure. Since the variation in the incremental displacement vector $\delta_t\{\Delta u\}^e$ is arbitrary, expressing the term within Ist parenthesis as linear elemental stiffness $[\,K_L\,]^e$ and that of 2nd one as nonlinear elemental stiffness $[\,K_{NL}\,]^e$ the above equation can be written as

$$ ({}_t[K_L]^e + {}_t[K_{NL}]^e)\ {}_t\{\Delta u\}^e + {}_t\{f\}^e = {}_{t+\Delta t}\{F\}^e \tag{2.76} $$

or

$$ {}_t[K]^e \, {}_t\{\Delta u\}^e + {}_t\{f\}^e = {}_{t+\Delta t}\{F\}^e. \tag{2.77} $$

where

$$ {}_t\{f\}^e = \int_{V_e^t} {}_t[B_L]^T \, \{\sigma\}^t \, \mathrm{d}V^t. \tag{2.78} $$

is the internal force vector.

Assembling the elemental matrices ${}_t[K]^e$ and the elemental vectors ${}_t\{f\}^e$ and ${}_{t+\Delta t}\{F\}^e$ over all the elements, we get the following global equation :

$$ {}_t[K] \, {}_t\{\Delta u\} + {}_t\{f\} = {}_{t+\Delta t}\{F\}. \tag{2.79} $$

Here ${}_t[K]$ is the global stiffness matrix, ${}_t\{\Delta u\}$ is the global incremental displacement vector (at time t) and ${}_t\{f\}$ and ${}_{t+\Delta t}\{F\}$ are the global internal and external force vectors respectively. Decomposing ${}_{t+\Delta t}\{F\}$, eq. (2.79) can be written as

$$ {}_t[K] \, {}_t\{\Delta u\} + {}_t\{f\} = {}_t\{F\} + {}_t\{\Delta F\}. \tag{2.80} $$

Here, ${}_t\{F\}$ is the (global) external force vector at time t and ${}_t\{\Delta F\}$ is the (global) incremental force vector from time t to $t + \Delta t$. In updated Lagrangian formulation, it is assumed that the equilibrium equations have been satisfied exactly at time t. Thus,

$$ {}_t\{f\} = {}_t\{F\}. \tag{2.81} $$

Then, eq. (2.80) reduces to

$$ {}_t[K] \, {}_t\{\Delta u\} = {}_t\{\Delta F\}. \tag{2.82} $$

Now, suppose we find the incremental stresses corresponding to the solution (${}_t\{\Delta u\}$) of eq. (2.82), add those to the earlier stresses to find the stresses at time $t + \Delta t$ and use eq. (2.78) to determine the internal force vector ${}_{t+\Delta t}\{f\}$ at time $t + \Delta t$, it is possible that it may not match with the applied (or external) force vector. Thus, eq. (2.82) represents only an approximate equilibrium equation at time $t + \Delta t$ (The approximation is mostly due to the linearization and simplification involved in the steps between eqs. 2.58 to 2.59). A solution of such an approximate equation may involve a significant amount of error and, depending on the time/incremental displacement step, may becomes unstable. Therefore, it is necessary to modify eq. (2.82) to turn it into an iterative problem capable of providing a solution with desirable accuracy. Newton Raphson scheme is one of the most commonly used technique to handle such nonlinearity.

2.3.4 Numerical Scheme

Normally we encounter two types of problems in mechanics: (1) Load control problem and (2) Displacement control problem. In a load control problem, the desired deformation is achieved by prescribing a load at a point. On the other hand, in a displacement control problem, it is the prescribed displacement which gives the desired deformation. In a load control problem, if the load falls due to change in geometry,then most iterative schemes fail to converge. Displacement control problems are free from this limitation. In this thesis, only displacement control problems are considered.

(I) The Newton Raphson Scheme

The scheme is best described with the help of Fig. (2.2) in the following steps. In Fig. (2.2), m is an equilibrium point at load level $\{P\}$. The aim is to reach another equilibrium point ($m+1$) at a load level ($\{P\}+\Delta\{P\}$).

Step 1 – First of all, the stiffness matrix ${}_t[K]$ in eq. (2.82) is evaluated using the stresses corresponding to point m. Next, eq. (2.82) is solved with ${}_t\{\Delta F\} = \{\Delta P\}$ to get an incremental displacement vector ${}_t\{\Delta u\}$.

Step 2 – From the incremental nodal displacements, incremental strain components are calculated by using eq. (2.2). Incremental stresses are calculated from the incremental strains by using suitable constitutive relation. Generally incremental stresses are calculated at the Gauss points of the elements. If the point under consideration is in elastic range, the elastic stress-strain matrix $[C]$ is used. Otherwise, elastic-plastic matrix $[C]^{EP}$ is used. Since elastic-plastic matrix is dependent on the current state of stress, the stress value at position m is used for the computation of elastic-plastic matrix. Eq. (2.23) is used to calculate Jaumann stress rate and the total Cauchy stress follows from eq. (2.24). *Step* 3 – Once the stresses are calculated at all the Gauss points of all the elements, the internal nodal force vector ${}_{t+\Delta t}\{f\}$ is calculated. This force corresponds to the equilibrium load at point i in Fig. (2.2).

Step 4 – Since the applied nodal forces $({}_t\{P\} + {}_t\{\Delta P\}$ are not equal to internal nodal forces ${}_{t+\Delta t}\{f\}$, the deformed configuration is not an equilibrium configuration at load level $({}_t\{P\}+{}_t\{\Delta P\})$. It gives rise to an unbalanced nodal forces $({}_t\{P\}+{}_t\{\Delta P\} - {}_{t+\Delta t}\{f\})$.

Step 5 – The steps 1 to 3 are repeated with unbalanced nodal forces as the load vector and i as a starting point. Successive repetition of the above steps will lead to the equilibrium point $(m+1)$ for load level ${}_t\{P\} + {}_t\{\Delta P\}$ when the unbalanced nodal forces become almost zero(less than a preassigned quantity). In each successive iteration ,incremental displacement vector is added to its previous value.

In full Newton-Raphson method, the stiffness matrix is updated after every iteration. This takes a lot of computational time per iteration but the number of iterations required for convergence, in one increment, is quite small. When one tries to reduce the computational time per iteration, it invariably increases the number of iterations per increment required for convergence. This may actually result in increasing the overall computational time per increment. The best compromise between the reduction in computational time per iteration and the increase in number of iterations per increment is offered by the modified Newton-Raphson method in which the stiffness matrix is modified only after the increment is over. The iterative scheme of the modified Newton-Raphson method can be described by the following equations:

$$ {}_t[K]_t\{\Delta u\}^{(i)} = {}_t\{R\}^{(i-1)} \qquad (2.83) $$

for i=1,2,3....

where ${}_t[K]$ is the same as in equation (2.82) and the right side vector is given by

$$ {}_t\{R\}^{(0)} = {}_{t+\Delta t}\{\Delta F\} \qquad (2.84) $$

$$ {}_t\{R\}^{(i)} = {}_{t+\Delta t}\{\Delta F\} - {}_{t+\Delta t}\{\Delta F\}^{(i)} \qquad (2.85) $$

for i=1,2,3....

However, this scheme creates some convergence problems for the rolling process. In this process, incremental deformation is simulated by prescribing incremental translation of the strip. While doing so, it must be ensured, in every increment, that a node exists at the entry to the roll gap. Thus, the minimum distance through which the strip can be advanced in one increment is the distance between two consecutive nodes on the top face. To achieve the convergence using the modified Newton-Raphson scheme, the incremental deformation has to be sufficiently small, but this will require a large number of elements and consequently a large number of dof. Solving a problem of such

a large size on IIT K computing systems takes a lot of time. To keep the problem at a manageable level, the element size has to be sufficiently big. This means the incremental deformation becomes large leading to convergence problem. To overcome this difficulty the following strategy is adopted. In this scheme, ${}_t[K]$ in equation (2.83) is replaced by the stiffness matrix updated after carrying out the first iteration. Then the modified Newton-Raphson method is applied using this new stiffness matrix.

(II) Scheme for divergence

If, during the iterations of modified Newton Raphson scheme, the unbalanced force vector in $(i+1)_{th}$ iteration increases compared to the unbalance force vector of i_{th} iteration, it means the scheme is diverging. This happens because we get a large value of ${}_t\Delta u^{(i+1)}$. In this situation, if magnitude of the stiffness matrix is increased and $(i+1)_{th}$ iteration is repeated, we can get a smaller value of ${}_t\Delta u^{(i+1)}$, and convergence can be achieved. If again there is divergence, the magnitude of the stiffness matrix can be increased again.

One way to increase the magnitude of the stiffness matrix is to add to it a fraction of the elastic stiffness matrix $[K]^E$ corresponding to that configuration. It is calculated using only the linear part of ${}_t[K]$ and replacing $[C]^{EP}$ by $[C]^E$. Thus, the modified stiffness matrix becomes

$$ {}_t[K]_{new} = (1-\alpha){}_t[K] + \alpha[K]^E \tag{2.86}$$

In this work, the above scheme is used to arrest the divergence, where α is found by numerical experiment.

(III) Euler Forward Integration Scheme In step 2 of modified Newton-Raphson scheme, if equation (2.31) is used to calculate the incremental stress vector where $[C^{EP}]$ is based on the current equilibrium configuration, then a lot of error occurs in estimating the stresses leading to a large value of unbalance. For better estimation of stresses, usually Euler Forward integration scheme is used. This scheme is described below.

- If the state at time t is elastic,

1. Evaluate strain increment using eq. (2.2) and Jaumann stress increment assum-

ing elastic behavior.

$$^{t}\{\Delta\sigma\} = [C^{E}]_{t}\{\Delta e\} \tag{2.87}$$

2. Evaluate Cauchy stress increment using eq. (2.24). Calculate $^{t+\Delta t}\{\sigma\}$

3. Determine $^{t}\sigma_{eq}$ and $^{t+\Delta t}\sigma_{eq}$ using eq. (2.5)

4. If $^{t+\Delta t}\sigma_{eq} \leq {}^{t+\Delta t}\sigma_{y}$ then elastic behavior holds. [If $^{t+\Delta t}\sigma_{eq} = {}^{t+\Delta t}\sigma_{y}$, the Gauss point is neutrally loaded]. **RETURN.**

5. If $^{t+\Delta t}\sigma_{eq} > {}^{t+\Delta t}\sigma_{y}$ a transition from elastic to plastic state has occurred. Calculate

$$Ratio = \frac{^{t+\Delta t}\sigma_{y} - {}^{t}\sigma_{eq}}{^{t+\Delta t}\sigma_{eq} - {}^{t}\sigma_{eq}} \tag{2.88}$$

and change the state to plastic. Calculate the Cauchy stress using the following procedure.

In each iteration, the sub-incrementation method is followed and the stress tensor components are updated after each sub-increment by adding the sub-incremental stress components corresponding to the elasto-plastic sub-incremental strain. First the $[C^{EP}]$ corresponding to the last updated state is calculated. Next, Jaumann stress increment for the sub-increment is evaluated. Then Cauchy stress increment is evaluated using eq. (2.24). Finally, the updated state of stress is evaluated: For i_{th} sub-increment, the Jaumann increment is given by

$$\overset{\circ}{\sigma}dt^{(i)} = {}^{t+\Delta t}[C^{EP}]^{(i-1)}d_{t}\{\Delta e\} \tag{2.89}$$

and the updated state of stress is obtained as

$$^{t+\Delta t}\{\sigma\}^{(i)} = {}^{t+\Delta t}\{\sigma\}^{(i-1)} + \{d\sigma\}^{(i)} \tag{2.90}$$

In the above equation,

$$^{t+\Delta t}\{\sigma\}^{0} = {}^{t}\{\sigma\} + Ratio[C^{E}]_{t}\{\Delta e\} \tag{2.91}$$

$$^{t+\Delta t}[C^{EP}]^{0} = {}^{t}[C^{EP}] \tag{2.92}$$

and $d_{t}\{\Delta e\}$ is obtained from the sub-incremental displacement

$$d_{t}\{\Delta u\} = \frac{(1 - Ratio)_{t}\{\Delta u\}}{n} \tag{2.93}$$

where n is the number of sub-increments.

Use above equations to find ${}^{t+\Delta t}\sigma_{ij}$. **RETURN.**

- If the state at time t is plastic, the sub-incrementation method in (5) above is applied with Ratio set to zero.

2.3.5 Unloading

The unloading has to be incorporated if one wants to get residual stresses in elasto-plastic deformation. The unloading criterion defined by Chakrabarty (1987) is implemented. According to this criterion, unloading occurs if

$$\{n\}^T\{\Delta\sigma\} < tolerance \tag{2.94}$$

where $\{\Delta\sigma\}$ is incremental stress vector and $\{n\}$ represents the unit outward normal to the yield surface at the current stress point ${}^t\{\sigma\}$ in a $9-D$ space. Neutral loading and positive loading are represented by replacing the "less than" symbol in above equation by the "equal to" and "greater than" symbols respectively. This unit normal to the yield surface is defined by

$$\{n\} = d\lambda\{de^p\} \tag{2.95}$$

where $d\lambda$ (> 0) is given by equation (2.11) and $\{de^p\}$ is incremental plastic strain vector.

When unloading is detected, the stress tag of Gauss point is changed from plastic to elastic and the increment is repeated. It is possible that during the repetition of the increment, the same Gauss point may again become plastic, but in that case it is not checked for unloading.

2.3.6 Choice of Shape Functions and Numerical Integration

Since the finite element method is a numerical procedure involving discretization of the domain, important considerations pertain to the convergence of the numerical solution with respect to mesh refinement. For monotonic convergence, the elements

must be *complete* and the elements and mesh must be *compatible.* If these conditions are fulfilled, the accuracy of the solution increases continuously as we continue to refine the finite element mesh. This mesh refinement should be performed by subdividing a previously used element into suitable number of more elements; thus, the old mesh must be " embedded " in the new mesh. *The requirement of completeness* of an element means that the polynomial approximating the displacements of the element must be able to represent the rigid body displacements and the constant strain fields. *The requirement of compatibility* means that the displacements within the element and across the element boundaries must be continuous.

Eq. (2.59) suggests that the convergence criterion will be satisfied if du_x and du_y are chosen to be bilinear functions of x and y. To satisfy the above condition, we have chosen the second order *Serendipity* approximation with eight nodded rectangular elements for the finite element formulation. Here, the term x^2y^2 of the assumed approximation polynomial is omitted because it increases the size and the bandwidth of the stiffness matrix without improving the approximation outside the element. The approximation is normally expressed in terms of the natural coordinates ξ and η. Thus, the shape functions N_i in eq. (2.68) are the second order *Serendipity shape functions* in ξ and η.

Exact evaluation of integrals appearing in element coefficient matrices and right side vectors is not always possible because of the algebraic complexity of the coefficients in differential equations. In such cases, it is natural to seek numerical evaluation of these integral expressions. Numerical evaluation of integrals, called numerical integration, involves approximation of the integrand by a polynomial of sufficient degree, because the integral of a polynomial can be evaluated exactly.

The most used numerical integration method is Gauss-Legendre numerical integration and formula for integrals defined over a rectangular master element Ω_R is given by

$$\int_{\Omega_R} F(\xi,\eta)\,\mathrm{d}\xi\,\mathrm{d}\eta = \int_{-1}^{-1}\left[\int_{-1}^{-1} F(\xi,\eta)\,\mathrm{d}\eta\right]\mathrm{d}\xi \tag{2.96}$$

$$\approx \sum_{i=1}^{m}\sum_{i=1}^{n} F(\xi_i,\eta_j)\,w_i\,w_j \tag{2.97}$$

where m and n denote the number of quadrature points (or the Gauss points) in the

ξ and η directions, (ξ_i, η_j) denote their natural coordinates, and w_i and w_j denote the corresponding weights.

2.4 Boundary Conditions

The typical boundary conditions can be classified as:

(i) *Geometric* or *essential* boundary conditions.
The incremental displacement vector du_i is specified at a point on the boundary.

(ii) *Force* or *natural* boundary conditions.
The incremental stress vector $\mathrm{d}t_i = \mathrm{d}\sigma_{ij}\, n_j$ is specified at a point on the boundary, where n_j represents the components of the unit outward normal vector.

Sometimes, we have mixed boundary conditions, i. e. at a point on the boundary, some components of incremental displacement vector and the remaining components of the incremental stress vector are specified.

The specific boundary conditions used in the rolling problem (Fig. 2.3) are given below.

1. **The top free surface before entry to roll gap(AB):** As stated earlier, the rolling process is simulated by specifying incremental displacements of some points on the strip. The points chosen are the 2 nodes on the boundary **AB** preceding the node **B**. At these points the boundary condition are

$$\mathrm{d}u_x = du_x^* \qquad \textit{Essential} \qquad (2.98)$$

$$\mathrm{d}u_y = du_y^* \qquad \textit{Essential} \qquad (2.99)$$

for node m, du_x^* is the difference in x coordinates of node B and node m and $du_y^* = 0$. For node n, du_x^* and du_y^*. are calculated from the condition that it should be on the roll surface.

Since AB is a free surface, at the remaining points of AB, the stresses can be specified to be zero. It is observed that no bulging occurs except near the roll entry. Therefore, to avoid bulging, the vertical incremental displacement

must be specified to be zero. Therefore, the following two conditions are chosen.

$$\mathrm{d}t_x \equiv \mathrm{d}\sigma_{xy} = 0 \qquad \textit{Natural} \qquad (2.100)$$

$$\mathrm{d}u_y = 0 \qquad \textit{Essential} \qquad (2.101)$$

2. **The roll-strip interface (BC):** The nodes on this boundary travel along the roll surface. Therefore the following boundary conditions are used.

$$\mathrm{d}u_x = du_x^* \qquad \textit{Essential} \qquad (2.102)$$

$$\mathrm{d}u_y = du_y^* \qquad \textit{Essential} \qquad (2.103)$$

where du_x^* and du_y^* are calculated from the mesh geometry.

3. **The top free surface after exit from roll gap(CD):** The boundary CD is a free surface. So, the stress components can be specified to be zero. but in order to avoid bulging of the boundary, y component of the incremental displacement is specified as zero. Thus, the two boundary conditions are

$$\mathrm{d}t_x \equiv \mathrm{d}\sigma_{xy} = 0 \qquad \textit{Natural} \qquad (2.104)$$

$$\mathrm{d}u_y = 0 \qquad \textit{Essential} \qquad (2.105)$$

4. **The front boundary (DE):** The boundary DE is a stress-free boundary. Therefore boundary conditions are

$$\mathrm{d}t_x \equiv \mathrm{d}\sigma_{xx} = 0 \qquad \textit{Natural} \qquad (2.106)$$

$$\mathrm{d}t_y \equiv \mathrm{d}\sigma_{xy} = 0 \qquad \textit{Natural} \qquad (2.107)$$

5. **The axis of symmetry, x-axis (EF) :** Because of symmetry, the y-component of incremental displacement and x-component of incremental stress vector are zero on EF. Therefore, the boundary conditions on EF are

$$\mathrm{d}t_x \equiv \mathrm{d}\sigma_{xy} = 0 \qquad \textit{Natural} \qquad (2.108)$$

$$\mathrm{d}u_y = 0 \qquad \textit{Essential} \qquad (2.109)$$

6. **The Entry Boundary (FA):** Boundary FA is a stress free boundary. Therefore, the boundary conditions are

$$\mathrm{d}t_x \equiv \mathrm{d}\sigma_{xx} = 0 \qquad \textit{Natural} \qquad (2.110)$$

$$\mathrm{d}t_y \equiv \mathrm{d}\sigma_{xy} = 0 \qquad \textit{Natural} \qquad (2.111)$$

2.5 Evaluation of secondary variables

As explained above, solution of the rolling problem is obtained in the form of nodal displacements and Gauss point stresses by solving equation (2.83). From these two sets of primary quantities, the secondary quantities like roll pressure, roll torque, residual stress distribution and contours of equivalent plastic strain are obtained residual stress, the shear and, normal stress distribution at the roll-strip interface, the stress and strain contours and roll torque are calculated.

The details of these calculations are explained briefly in the following lines.

i. Roll pressure or inter-facial normal stress:

Using the values of σ_{ij} at the Gauss points, first they are extrapolated to the nodes at the roll-strip interface, then normal stress t_n is evaluated as

$$t_n = t_i n_i \tag{2.112}$$

where

$$t_i = \sigma_{ij} n_j \tag{2.113}$$

and n_j is unit outward normal to the interface.

ii. Roll torque:

Roll torque is calculated as:

$$T = \Delta W / \Delta\theta \tag{2.114}$$

where $\Delta\theta$ is incremental angle of rotation of roll and ΔW is total work involved in the increment, which consists of the work of deformation and the work to overcome friction (front and back tensions assumed to be zero).

Work of deformation is calculated using the Cauchy stress and linear incremental strain. Thus,

$$\Delta W_{deformation} = \int_V \sigma_{ij} \Delta\epsilon_{ij} \mathrm{d}V \tag{2.115}$$

Work to overcome friction is given by

$$\Delta W_{friction} = \int_S t_s (R\Delta\theta - \Delta u_s) \mathrm{d}s \tag{2.116}$$

where R is the roll radius, Δu_s is the tangential displacement and t_s is the shear stress at the roll strip interface. The shear stress is calculated from

$$|t_s| = \mu |t_n| \tag{2.117}$$

where μ is the coefficient of friction. The sign of t_s is determined by using the following expression (with out the tensions) for the neutral point which is based on the slab method [Bland and Ford(1948)].

$$tan^{-1}\sqrt{\frac{R}{h_2}}\phi_n = \frac{1}{2}sin^{-1}(\sqrt{r}) - \frac{1}{4a}ln\{\frac{h_1}{h_2}\} \tag{2.118}$$

where

ϕ_n = location of neutral point.

h_1 = initial thickness of the strip.

h_1 = final thickness of the strip.

r = percentage reduction.

The parameter a is given by,

$$a = \mu\sqrt{\frac{R}{h_2}} \tag{2.119}$$

iii. Residual stress distribution:

Distribution of residual stress components is first obtained over the domain in the form of contours. The contours are plotted from their Gauss point vaues using a standard technique. Then, the variation of residual stresses over the thickness is obtained from these contours.

iii. Contours of equivalent plastic strain:

These contours are also obtained from the Gauss point values using a standard technique.

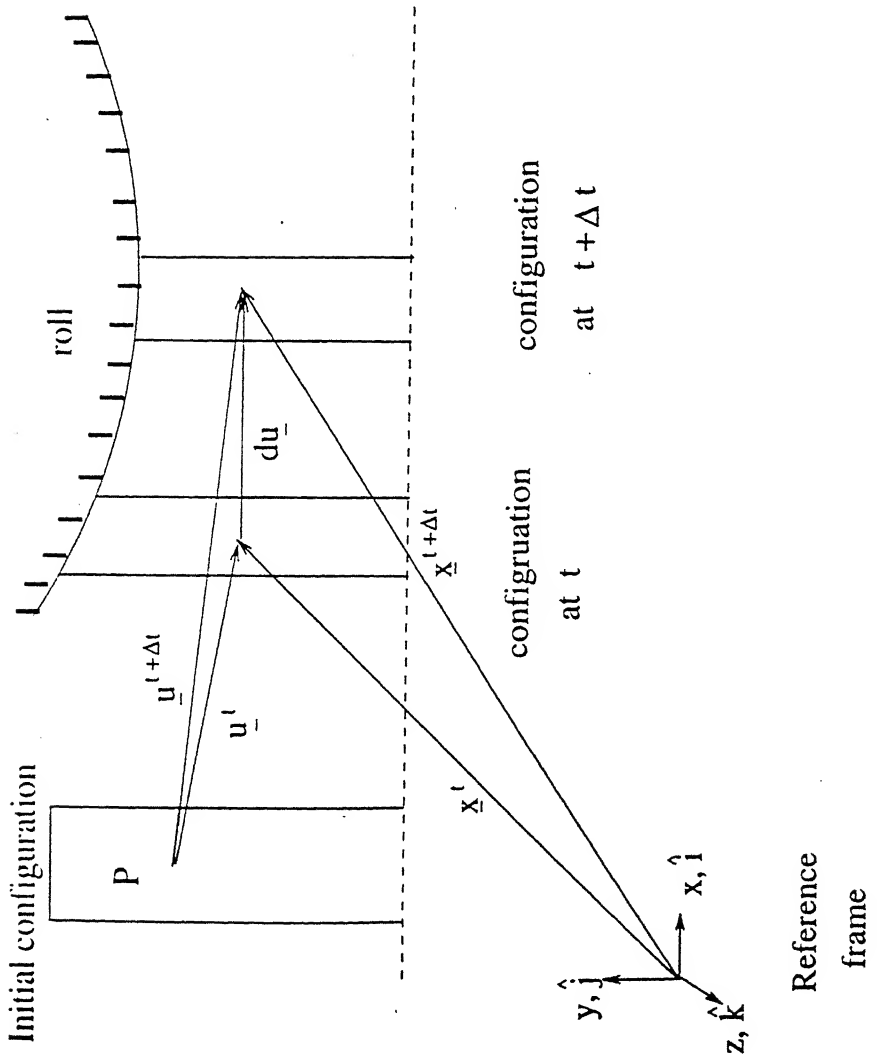

Figure 2.1: Various configuration of an element of the strip being rolled

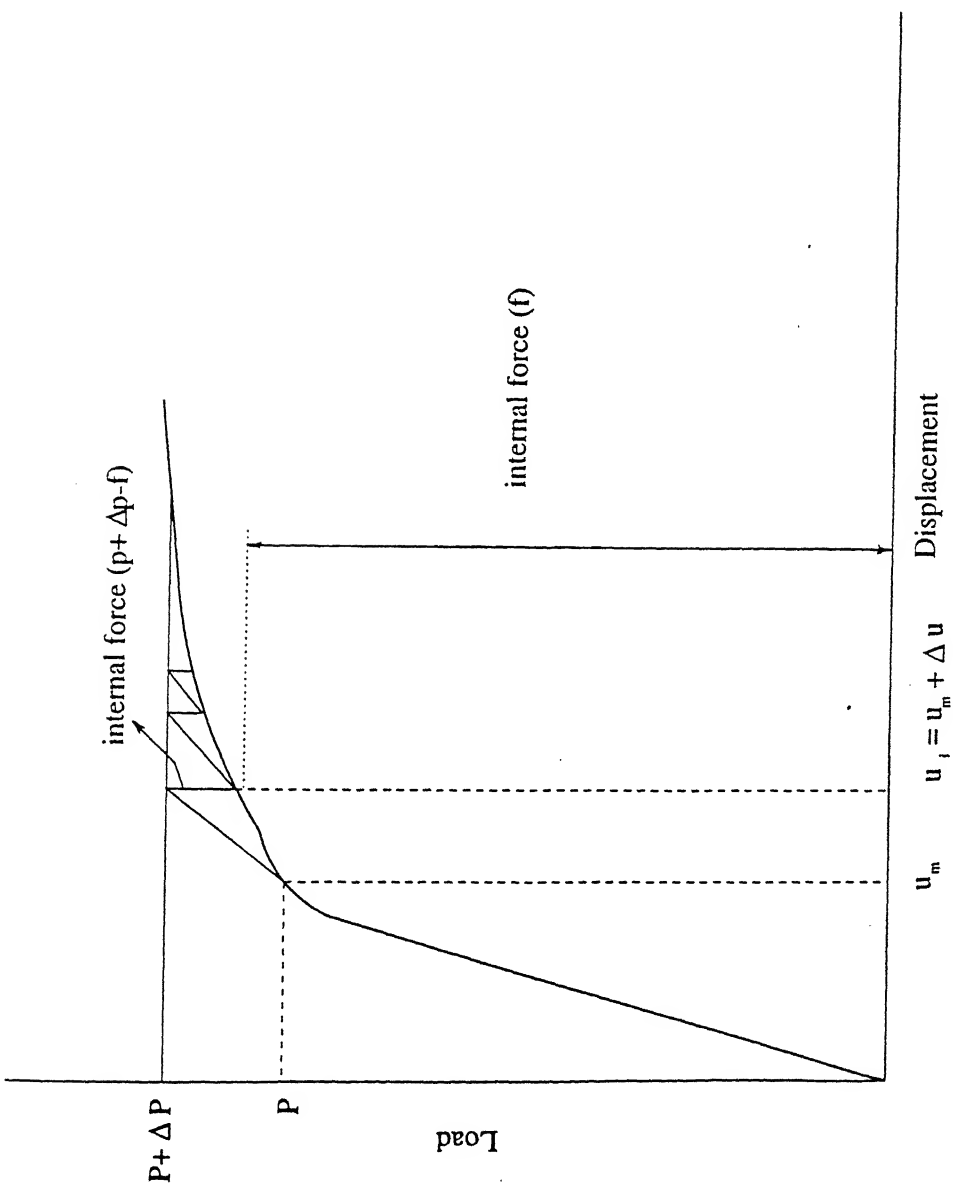

Figure 2.2: Illustration of Newton Raphson iterative scheme for a single load

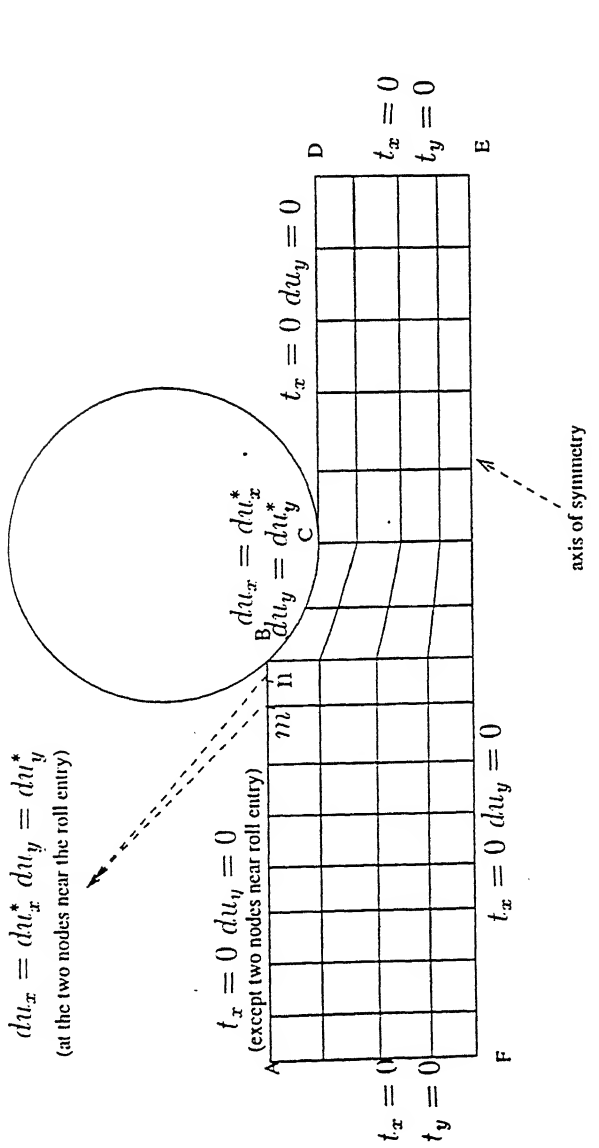

Figure 2.3: Mesh and boundary conditions in strip rolling

Chapter 3

Results And Discussion

The finite element modeling of cold strip rolling process developed in the previous chapter has been applied to various sets of input variables. The metal considered is hot rolled and annealed steel AISI 4140, the material properties of which are given in Table 3.1 [Reddy et al (1995)].

Young' modulus	:	210 GPa
Poisson's ratio	:	0.3
Initial yield stress	:	418.9 MPa
Hardening coefficient	:	699.0 MPa
Hardening exponent	:	0.266

Table 3.1: Material properties of AISI 4140 steel.

The value of 0.08 is used for the coefficient of friction μ to determine the friction work in equation (2.116).

First the model is validated. Then residual stresses and plastic strain are presented for one typical case in the next section. Parametric study is done by changing the parameters R/h_1 and % reduction. In all the cases, the initial thickness of the strip is kept constant.

The mesh data for the various cases is given in Table 3.2 below.

reduction(%)	R/h_1	elements	No. of nodes
5	130	272	961
5	65	248	877
15	65	348	1227

Table 3.2: Mesh data for various cases.

3.1 Validation of the model

For validation of the model, the results are compared with the predictions of the Rigid-plastic Eulerian formulation of Dixit and Dixit (1996). Table 3.3 shows the comparison of roll torque with that found by Dixit (1997) based on the formulation of Dixit and Dixit (1996). It can be seen that the agreement is good with the error being 6%. It is to be noted that whereas the Eulerian formulation gives only the steady-state value of torque, the updated Lagrangian formulation gives the information about how the torque varies as the strip advances. This variation is exhibited in section 3.4 on parametric study (see Fig 3.12).

Present work	:	1.391 kN-m/m
Dixit(1997)	:	1.479 kN-m/m

Table 3.3: Comparison of roll torque per unit width ($r = 5\%, R/h_1 = 65$).

Figure 3.1 shows the comparison of normal stress distribution with that of Dixit (1997). The predicted values are lower than that of Dixit (1997) because the roll deformation has been neglected in the present work. Whereas the distribution is more or less uniform in case of Dixit (1997), the present work shows 2 peaks, the entry peak being smaller than the exit peak. This difference is also due to the assumption of rigid rolls.

3.2 Residual stresses and strain

Figures 3.2 - 3.4 show contours of stress components σ_{xx} & σ_{xy} and equivalent plastic strain e^p_{eq} for a typical case of $r = 5\%$ and $R/h_1 = 65$. It can be seen that, when the strip travels a sufficient distance ($> 3h_2$) from the roll exit, the stresses and strain

remain more or less constant, except of course at the end because of the free surface effect. These represent the residual stresses and strain in the strip.

Figures 3.5 - 3.7 show the variations of steady-state values of σ_{xx} & σ_{xy} and e^p_{eq} along the thickness. It can be seen from Fig 3.5 that the longitudinal residual stress (σ_{xx}) is positive at the top surface whereas it is negative at the center. Similar trend has been reported by Dixit and Dixit (1997) who have used a simplified method based on Eulerian formulation to determine the residual stresses. Our values cannot be compared directly with their values as their results are for higher reduction. Figure 3.5 shows that shear residual stress (σ_{xx}) is very small compared to longitudinal residual stress (σ_{xx}). The equivalent plastic strain (e^p_{eq}) is observed to be more at top fibers than at the center (Fig 3.7). This shows that the assumption of homogeneous deformation, often made in elementary method of analysis is not valid at least for the case of low reduction.

3.3 Deformed Configuration and Plastic Boundaries

Figure (3.8 a) shows the deformation pattern at the front end while Figure (3.8 b) shows the same at the roll exit. These figures show the deformed position of an initially straight cross-section of the strip. The pattern is different at the front end because of the free surface effect. The pattern at the roll exit is consistent with the distribution of longitudinal stress (σ_{xx}) along the thickness (Fig 3.5). Figure (3.8 b) shows that the elongation of top fibers is less than that of central fibers. It means, the unloading has to be more for the central fibers to maintain the compatibility in steady-state. Whereas the unloading for the top fibers results in retaining a part of the positive elastic strain (e_{xx}), the unloading for the central fibers continues beyond the zero value so as to acquire the negative elastic strain (e_{xx}). This phenomenon explains why the residual stress are positive in the top fibers and negative in the central fibers.

Figure (3.9) shows the plastic boundaries. The front boundary is the first nonzero contour of e^p_{eq} and indicates the onset of plastic deformation. The second boundary indicates the beginning of unloading. Beyond this boundary, there is no change in the values of e^p_{eq} and therefore the contour pattern remains the same.

3.4 Parametric Study

In this section, the effects of process variables of % reduction and R/h_1 ratio are analyzed on residual stress and strain, roll torque and normal stress at the roll-strip interface. While analyzing these effects, the initial thickness of the strip and the friction coefficient are kept constant. Figures 3.10 - 3.13 show the effects of % reduction and R/h_1 on σ_{xx}, e^p_{eq},roll torque and normal stress respectively.

3.4.1 Effect of Change in R/h_1 Ratio

Figure 3.10 shows that even though the distribution pattern along the thickness remains the same, the values of longitudinal residual stress (σ_{xx}) decrease with R/h_1 ratio. This happens because the deformation (especially the change of length in longitudinal fibers) becomes more homogeneous with the increase in roll radius. The distribution of e^p_{eq} (both the pattern as well as values), however, seems to be in sensitive with R/h_1 ratio (Fig 3.11). The roll torque increases with R/h_1 ratio (Fig 3.12) because the arc-length increases with roll radius. Figure 3.13 shows that the pattern of normal stress distribution doesn't change with R/h_1 ratio. However, the values decrease. This may be because, now, the deformation is more homogeneous.

3.4.2 Effect of Change in % Reduction

More reduction means more deformation. As a result, even though the distribution pattern remains the same, the values of σ_{xx} (Fig 3.10), e^p_{eq} (Fig 3.11), roll torque (Fig 3.12) and normal stress (Fig 3.13) increase.

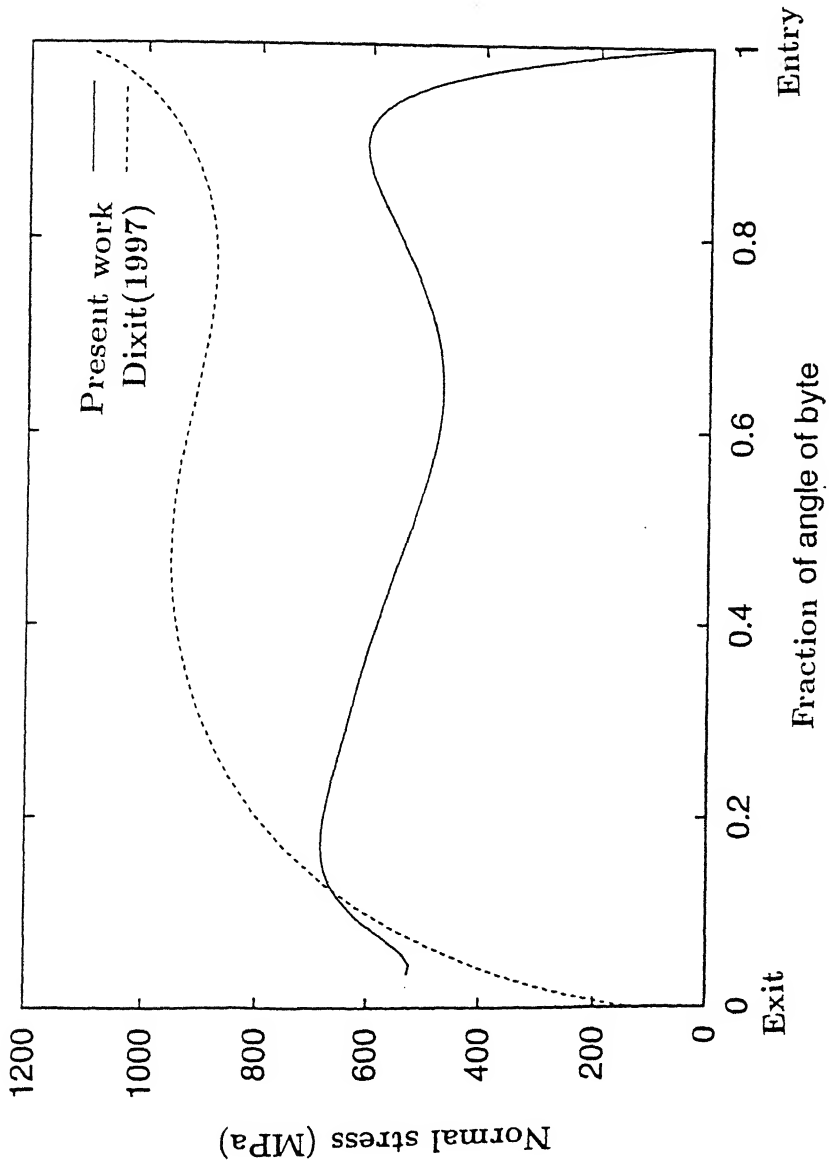

Figure 3.1: Comparison of normal stress distribution along the roll-strip interface

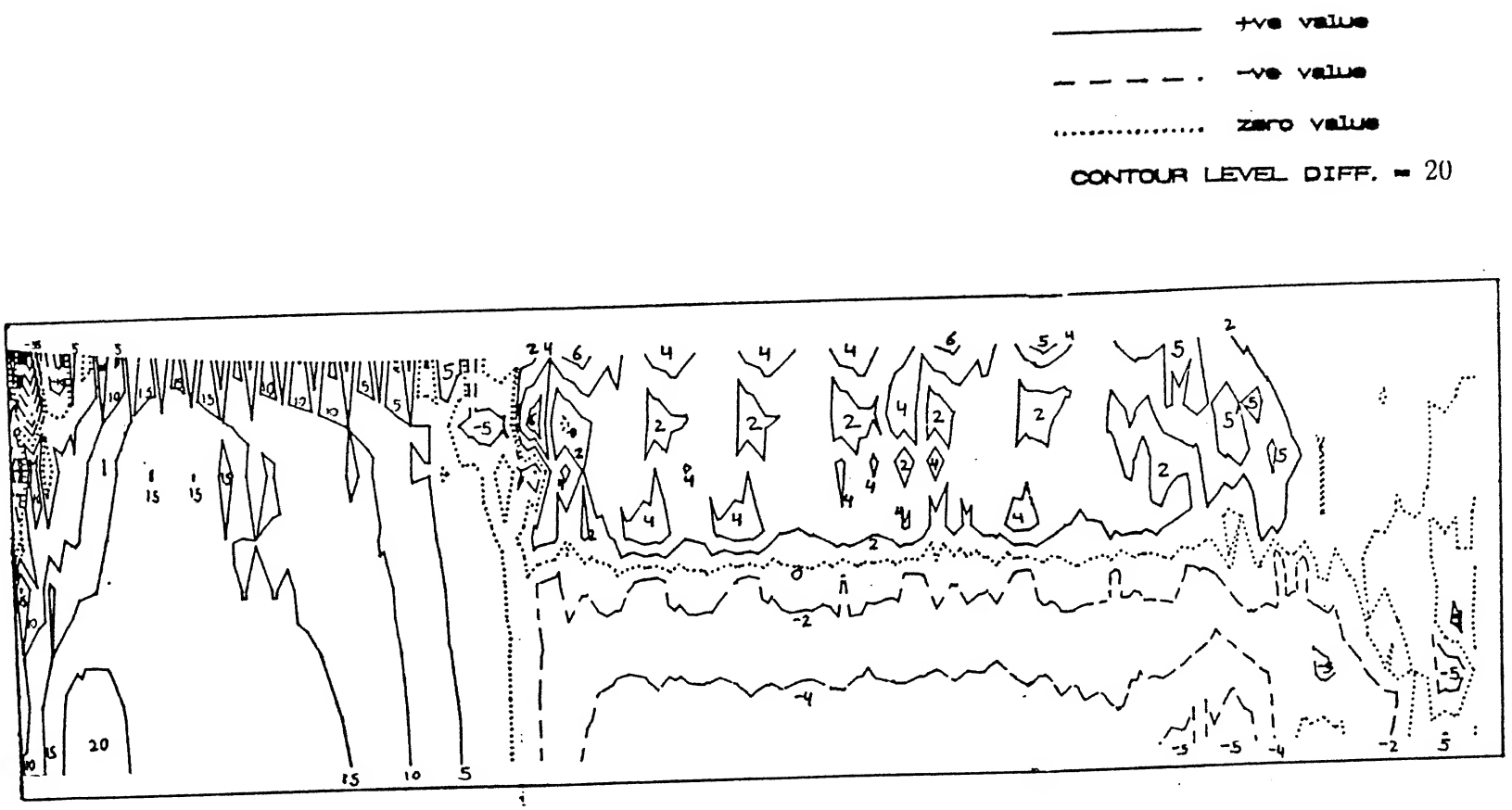

Figure 3.2: Contours of σ_{xx} for one typical case of 5% reduction and $R/h_1 = 65$

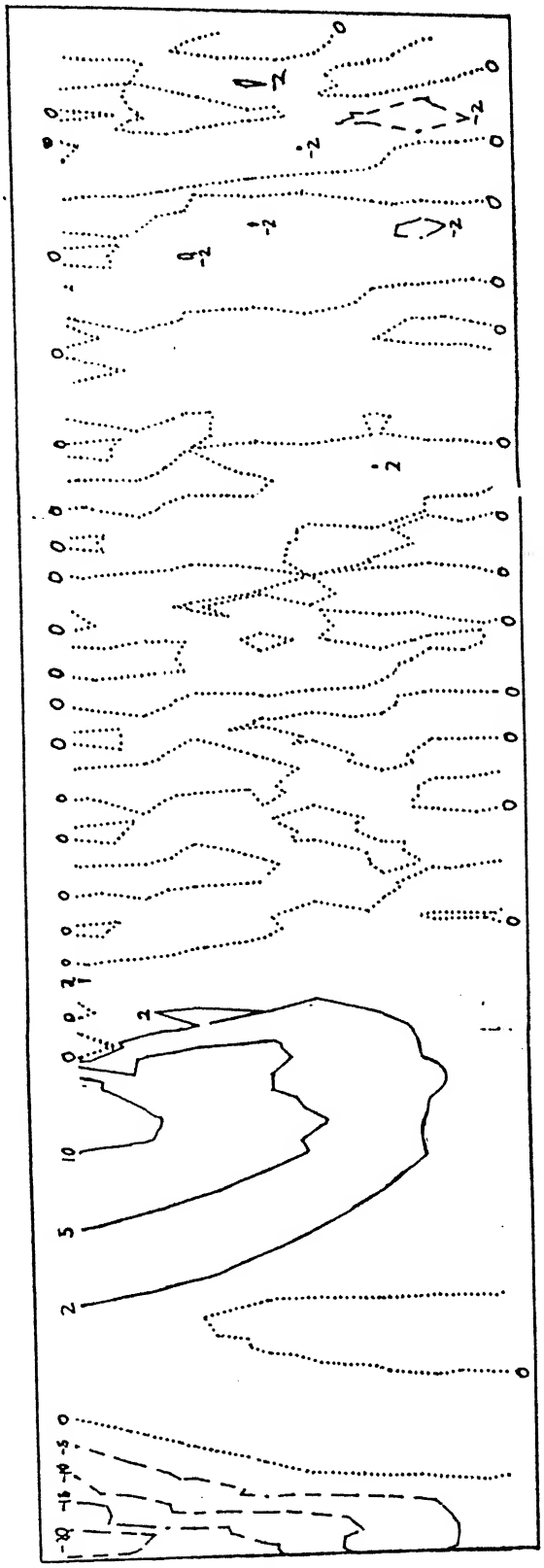

Figure 3.3: Contours of σ_{xy} for one typical case of 5% reduction and $R/h_1 = 65$

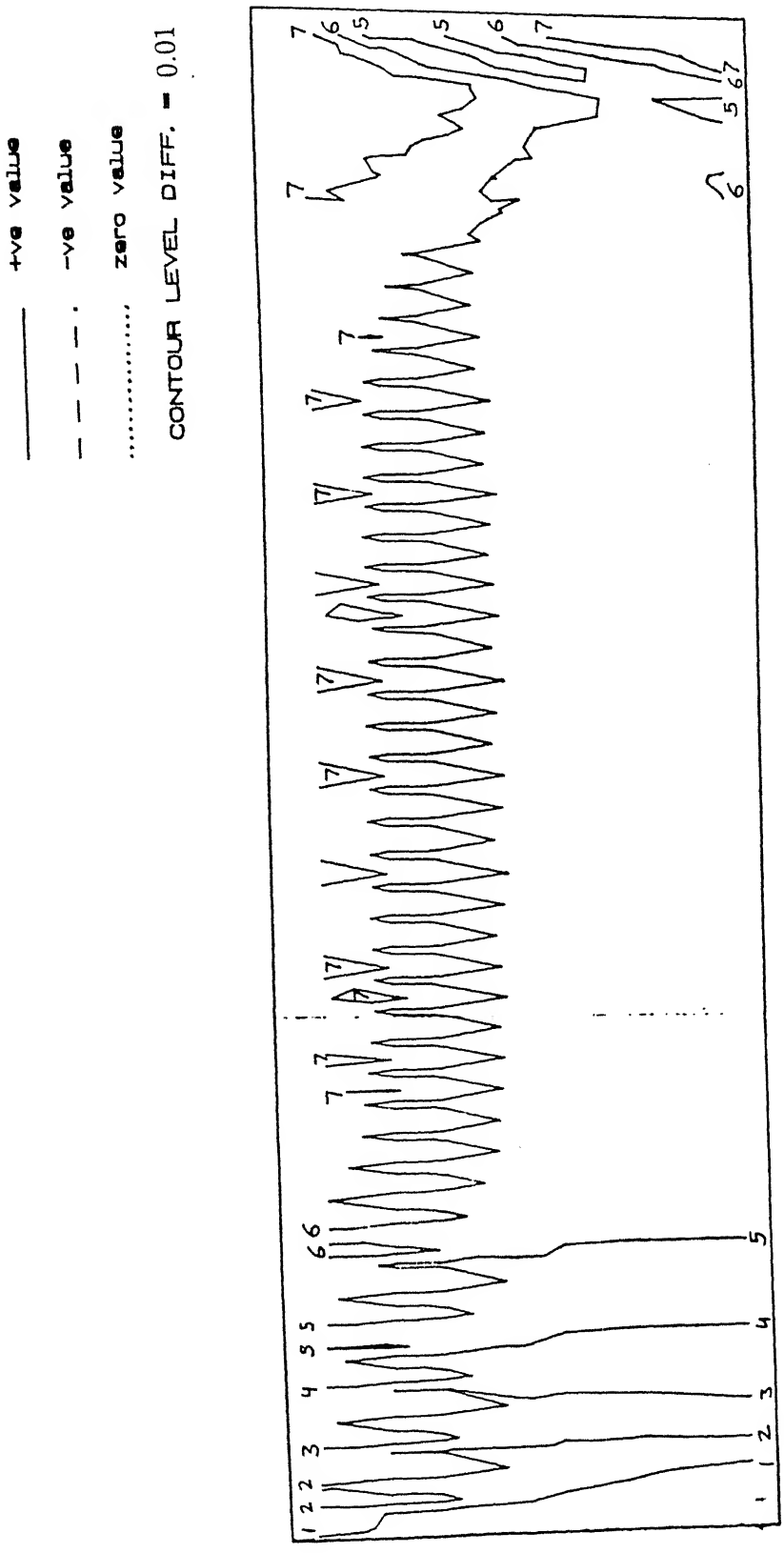

Figure 3.4: Contours of e_{eq}^{p} for one typical case of 5% reduction and $R/h_1 = 65$

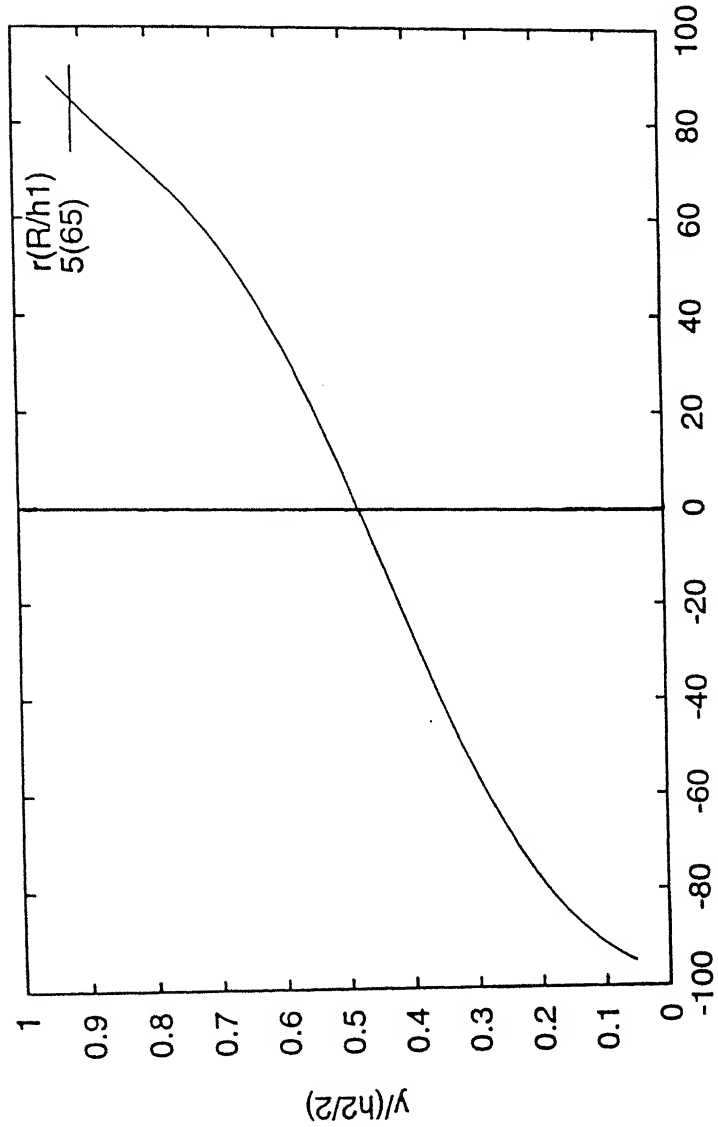

Figure 3.5: variation of σ_{xx} along thickness, for one typical case of 5% reduction and $R/h_1 = 65$

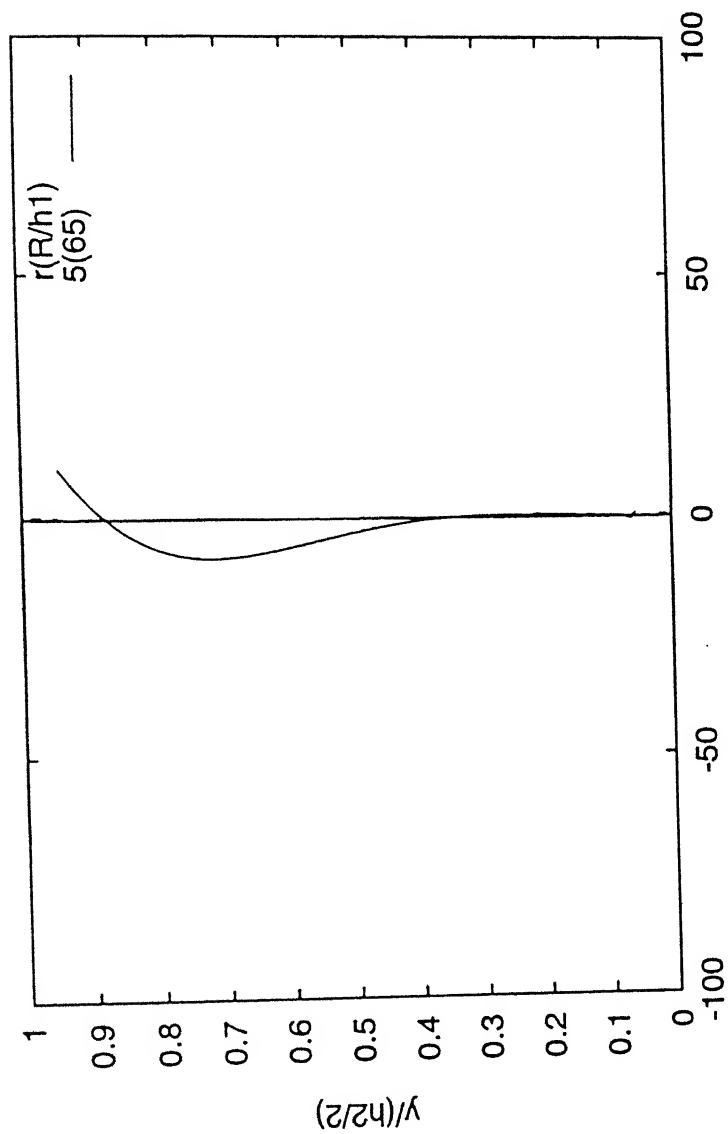

Figure 3.6: Variation of σ_{xy} along thickness, for one typical case of 5% reduction and $R/h_1 = 65$

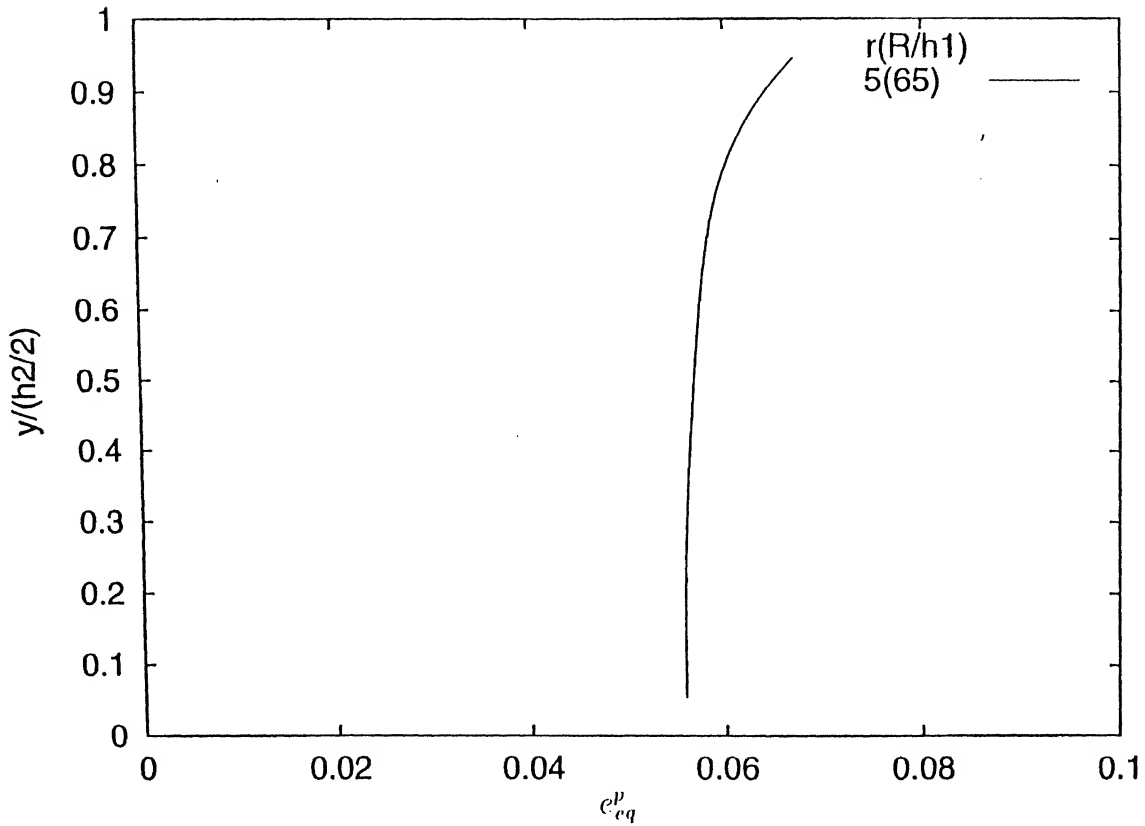

Figure 3.7: Variation of e^p_{eq} along thickness, for one typical case of 5% reduction and $R/h_1 = 65$

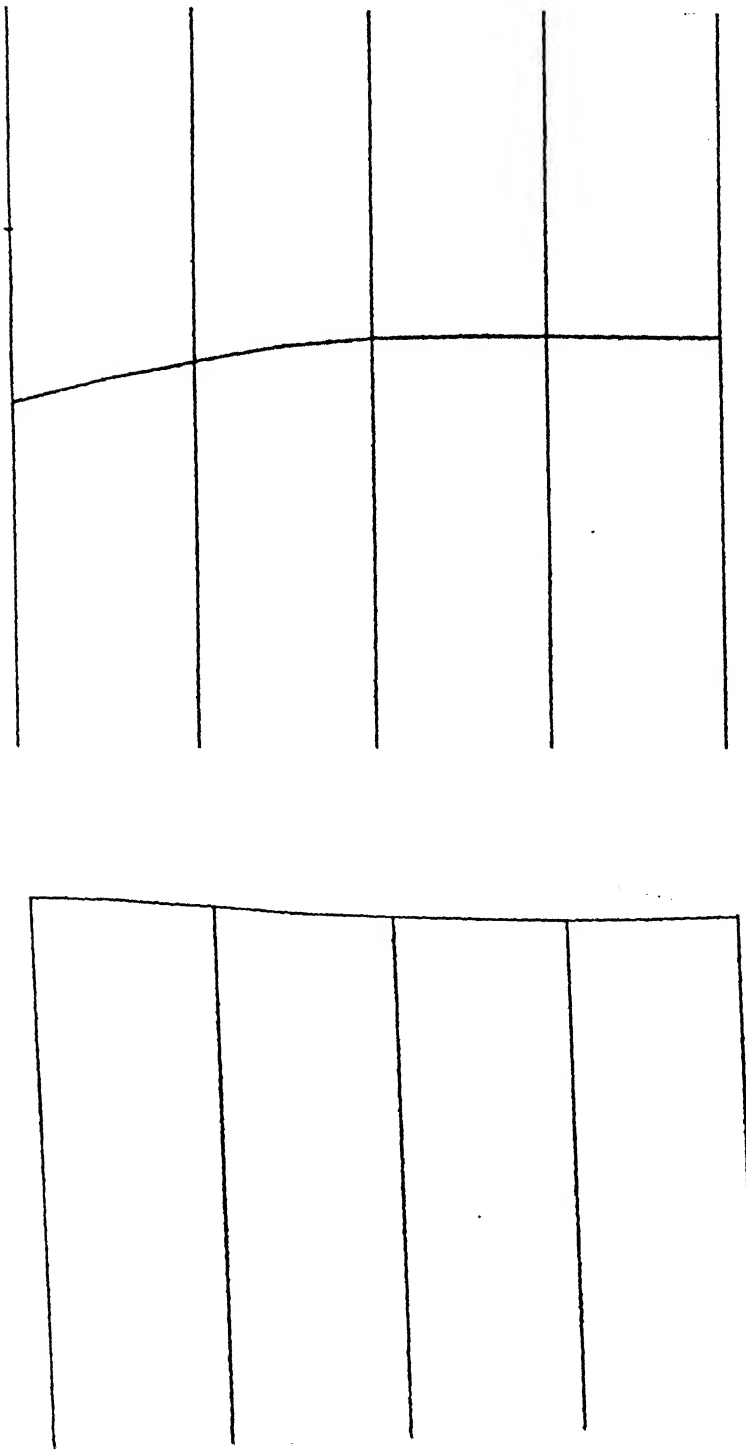

Figure 3.8: (a) Deformation pattern at front end (b) Deformation pattern at roll exit

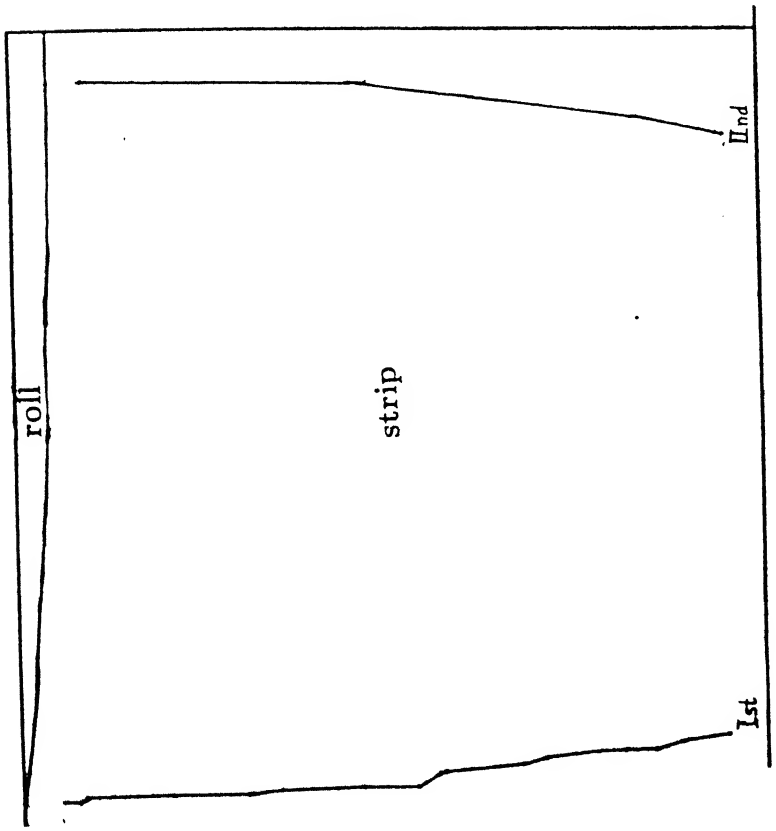

Figure 3.9: Plastic boundaries

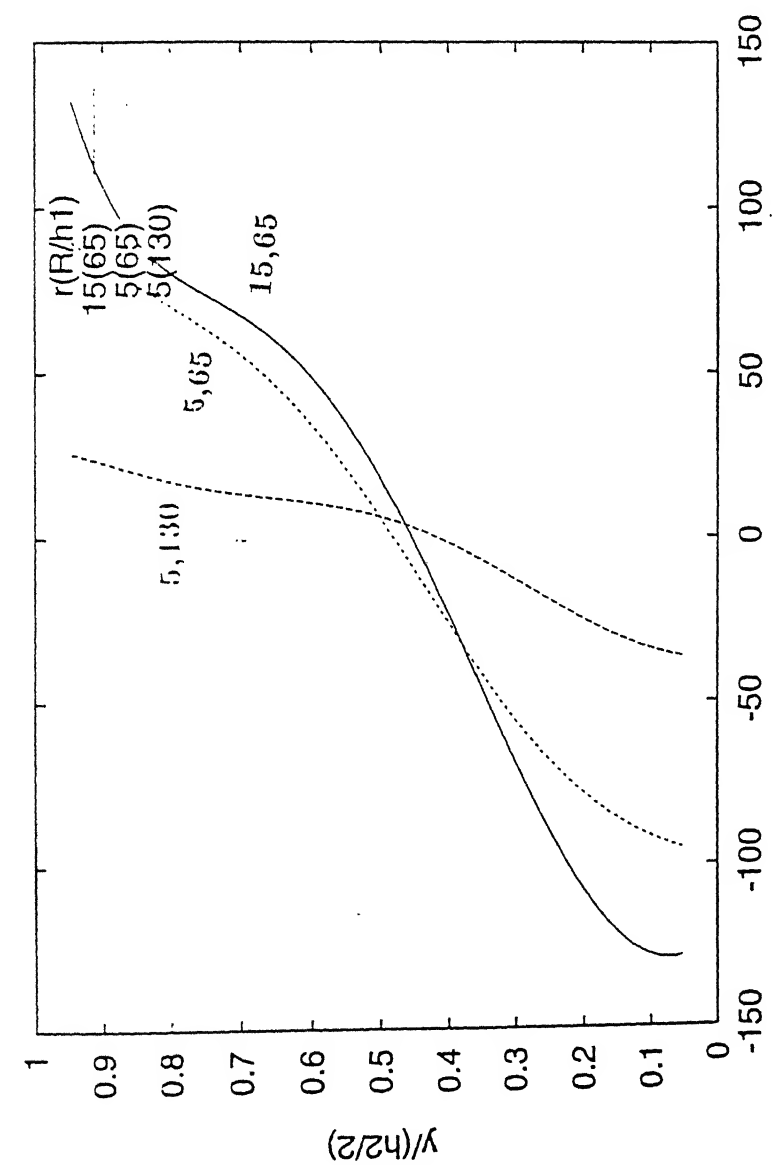

Figure 3.10: variation of σ_{xx} along thickness for various cases

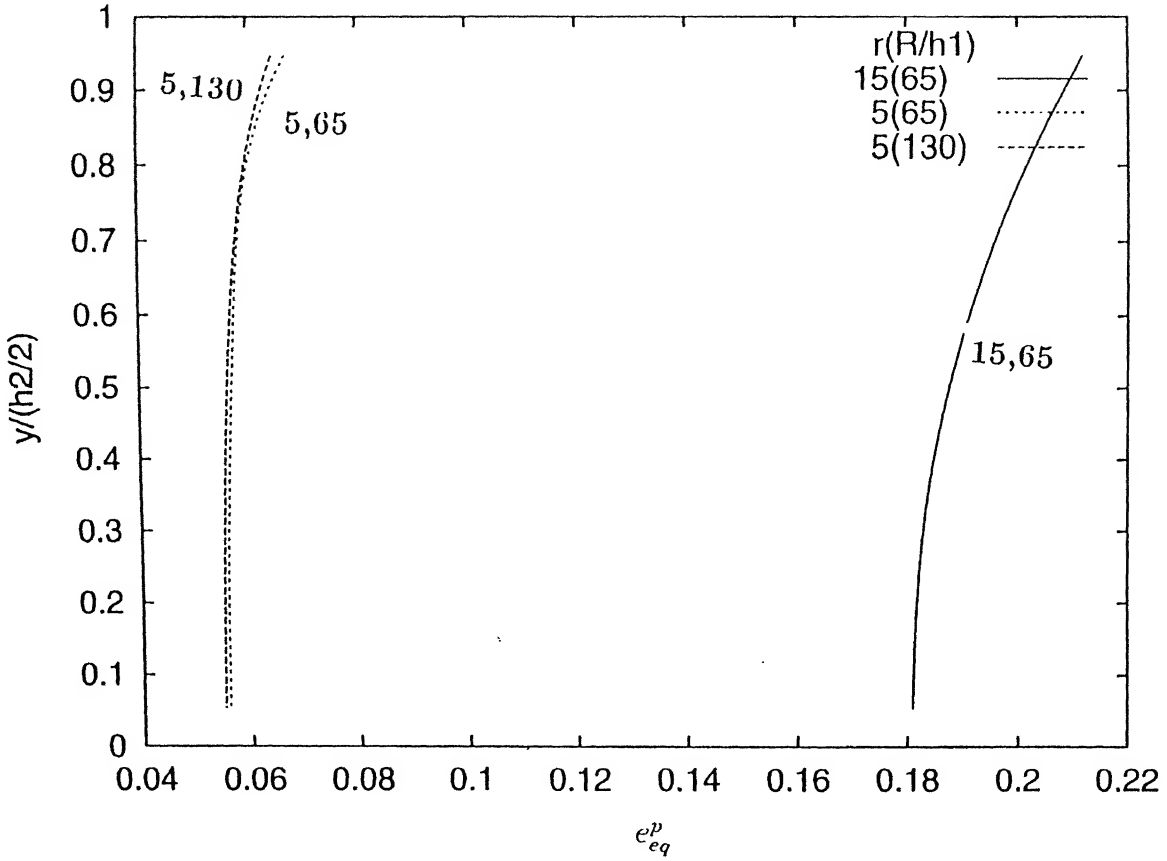

Figure 3.11: Variation of e^p_{eq} along thickness for various cases

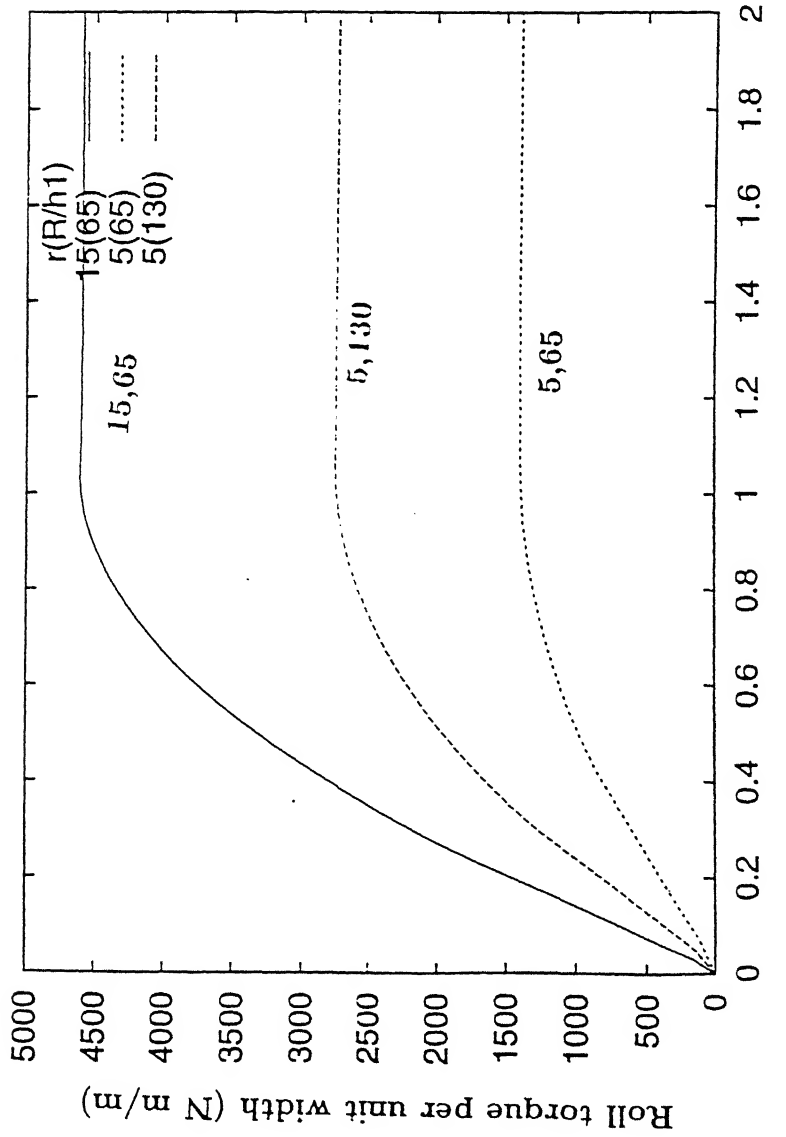

Figure 3.12: Variation of roll torque with increment.

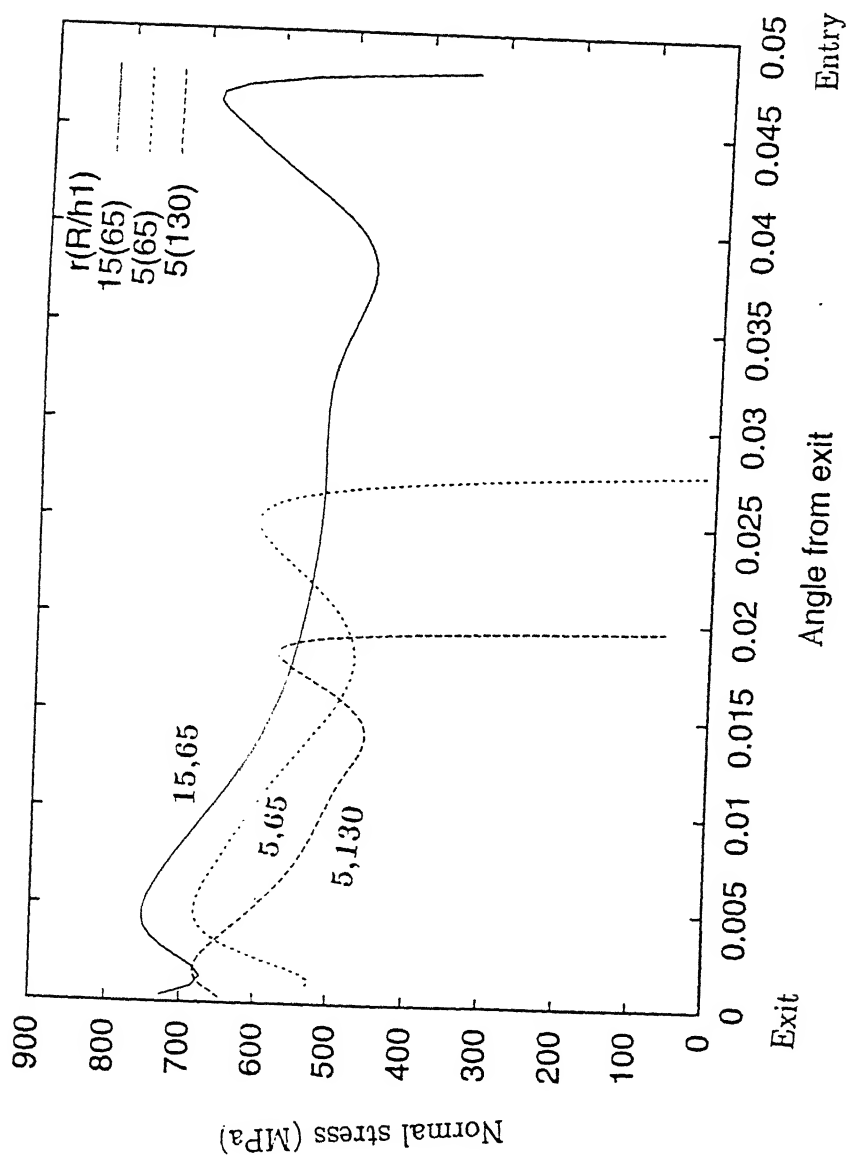

Figure 3.13: Variation of normal stress versus angle from exit, for various cases

Chapter 4

Conclusions and Suggestion for Further Work

4.1 Conclusions

Present work is an attempt towards determination of residual stresses in plane strain cold rolling. Even though an Eulerian formulation is a natural formulation for a steady-state process like rolling, there are unsolved difficulties with the convergence of elasto-plastic Eulerian formulation. Therefore an updated Lagrangian formulation is used. A large deformation elasto-plastic finite element code has been developed for the determination of residual stresses. The code predicts that the shear component of residual stresses (σ_{xy}) is negligible which is along expected lines. The thickness wise distribution of longitudinal residual stress (σ_{xx}) matches qualitatively with the published results. Thus, the code is successful in evaluating σ_{xx} and σ_{xy} components of the residual stresses. However, very high values of σ_{yy} are predicted which is contrary to the expectation. In fact σ_{yy} also should be of the order of σ_{xy}. The reason for high values of σ_{yy} is improper modeling of the boundary condition on the free surface after the roll exit. The condition used in the present work is $du_y = 0$ whereas more appropriate condition is $ty = 0$. However, when this condition was tried, certain numerical difficulties were encountered, which could not be overcome during the available time. But, certain suggestions to overcome the problem are offered in the next section.

4.2 Suggestions for Further Work

- *Evaluation of σ_{yy} :*

  As stated above, for proper evaluation of σ_{yy}, the boundary condition on the top surface (after the roll exit) should be $ty = 0$ instead of $du_y = 0$. However, when this condition was applied, the vertical incremental displacements of the nodes in the vicinity of the roll become so large that they penetrated the roll. This is not possible physically. For such nodes, the increment has to be repeated using the condition on vertical incremental displacement which now would be equal to the distance of the node from the roll surface. The finite element code should be modified to incorporate this feature for the nodes leaving the roll gap.

- *Inclusion of Inertial forces :*

  Inertial forces cannot be neglected during start up of the process. During the start-up, some non-zero stresses are developed in the entry region. Further, the roll torque during start-up is more than the steady-state value. These features can be simulated if inertia forces are included. Provision can be made to include the inertia forces only during start up, i.e. till the roll torque reaches a steady value.After that inertia forces need not to be included.

- *Friction boundary condition :*

  In the present work, the friction coefficient has been used indirectly in the calculation of roll torque. This is because the shear stresses at the roll-strip interface are not predicted accurately by the present model. For this purpose, the constant friction law can be used as one of the boundary condition.

- *Roll deformation :*

  The prediction of normal stress distribution at the roll-strip interface can be improved by incorporating roll deformation. This can be done using Hitchcock's formula as it is simple.

References

1. Abo-Elkhier, Oravas G. A. E. and Dokainish M. A., 1988, A consistent Eulerian formulation for large deformation analysis with reference to metal extrusion process, *Int. J. Non-Linear Mech.* **23**, 37-52.

2. Bathe, K. J., Ramm, E. and Wilson, E. L., 1975,Finite Element Formulations for Large Deformation Dynamics Analysis, *Int. J. Numer. Methods Engng* **9**, 353-386.

3. Bland, D. R. and Ford, H., 1948, The claculation of roll force and torque in cold strip rolling with tension, *Proc. Instn Mech. Engr*, **159**, 144-153.

4. Chakrabarty, J., 1987, Theory of Plasticity, *McGraw-Hill Book Company*, New Delhi.

5. Dawson P.R. and Thompson E.G.,1978, Finite element analysis of steady-state elasto-visco-plastic flow by the initial stress rate method, *Int. J. Numer. Methods Engng* **12**, 47-57.

6. Dixit U. S., 1997, *Private communication.*

7. Dixit U. S., Dixit, P. M., 1996, A finite element analysis of flat rolling and application of fuzzy set theory, *Int. J. Mech. Tools Manufact*, **36**, 947-969.

8. Dixit U. S., Dixit, P. M., 1997, A study on residual stresses in rolling, *Int. J. Mech. Tools Manufact*, **37**, 837-853.

9. Hart E.W., 1976, Constitutive relation for inelastic deformation of metals, *ASME J. Engng Mat. Tech.* **98**, 193-202.

10. Hill, R., 1950, The mathematical theory of plasticity, *Clarendon Press, Oxford.*

11. Liu, C., Hartley, P., Sturgess, C.E.N. and Rowe, G. W., 1985a, Elastic-plastic finite element modeling of cold rolling of strip, *Int. J. Mech. Sci.,* **27**, 531-541.

12. Liu, C., Hartley, P., Sturgess, C. E. N. and Rowe, G. W., 1985b, Simulation of the cold rolling of strip using an elastic-plastic finite element technique, *Int. J. Mech. Sci.,* **27**, 829-839.

13. Malinowski, Z., 1993, Elastoplastic finite element solution to the stress problem in the plane-strain cold rolling process, *Metallurgy and Foundry Eng.,* **19**, 323-336.

14. Malinowski, Z. and Lenard, J. G., 1993, Experimental substantiation of an elasto-plastic finite element scheme for flat rolling, *Comput. Methods Appl. Mech. Eng.,* **104**, 1-17.

15. Maniatty, A. M., 1994, Predicting Residual stresses in steady-state forming processes, *Computing Systems Eng.,* **5**, 171-177.

16. Maniatty, A. M., Dawson, P. R. and Weber, G. G., 1991, An Eulerian Elasto-Viscoplastic Formulation for Steady-State Forming Processes", *Int. J. Mech. Sci.*, **33**, 361-377.

17. Owen, D. R. J. and Hinton, E., (1980) *"Finite Elements in Plasticity: Theory and Practice,"* Pineridge Press, Swansea, UK.

18. Reddy N. V., Dixit P. M., Lal G. K., 1995, Die design for axi-symmetric extrusion, *J. Mater. Process Technol.***55**, 331-339.

19. Shimazaki Y. and Thompson E.G.,1981, Elasto-visco-plastic flow with special attention to boundary conditions, *Int. J. Numer. Methods Engng* **17**, 97-112.

20. Thompson, E. G. and Berman, H. M., 1984,Steady-state analysis of elasto-visco-plastic flow during rolling, in J.F.T. pittman *et al.(eds.), Numerical Analysis of Forming Processes,* Wiley, New York, 269-283.

21. Thompson, E. G. and Yu, S., 1990, A flow formulation for rate equilibrium equations, *Int. J. Numer. Methods in Engng,* **30**, 1619-1632.